2017-06-01

Sedimentology and Taphonomy of the *Abydosaurus mcintoshi* Quarry, (Naturita Formation, Early Cretaceous, Latest Albian), Dinosaur National Monument, Utah

Aaron Daniel Holmes
Brigham Young University

Sedimentology and Taphonomy of the *Abydosaurus mcintoshi* Quarry, (Naturita Formation, Early Cretaceous, Latest Albian), Dinosaur National Monument, Utah

Aaron Daniel Holmes

A thesis submitted to the faculty of
Brigham Young University
in partial fulfillment of the requirements for the degree of

Master of Science

Brooks Britt, Chair
Sam Hudson
Scott Ritter

Department of Geological Sciences

Brigham Young University

ABSTRACT

Sedimentology and Taphonomy of the *Abydosaurus mcintoshi* Quarry,
(Naturita Formation, Early Cretaceous, Latest Albian),
Dinosaur National Monument, Utah

Aaron Daniel Holmes
Department of Geological Sciences, BYU
Master of Science

The holotypic locality of the brachiosaurid titanosauriform sauropod, *Abydosaurus mcintoshi*, is quarry DNM-16, located in Dinosaur National Monument. The bones are preserved near the base of a heterolithic, trough cross stratified to planar bedded sandstone channel complex. The trough cross to planar bedded sandstones mark times of variable flow with times of high flow velocity based on bones whose upper surfaces were eroded before final burial. The abundance of mud with the dominant medium to fine sand, and poorly confined sandstone channels indicate the bones were transported and buried in medial to distal intermittent flows of a distributive fluvial system.

The quarry is at the base of the Naturita Formation, the base of which is latest Albian in age. The sauropods lived and died in the middle Cretaceous as the Cretaceous seaway advanced southward. The unconformity below the Naturita Formation and on top of the underlying the Ruby Ranch Member represents the LK-2 sequence boundary.

The quarry produced ~260 bones, all of which represent *Abydosaurus,* except for several small theropod teeth, denoting a single catastrophic event acting on a group of sauropods. About one-third of the bones occur in close association or articulation, including three skulls (one articulated with the first five cervical vertebrae), five limbs, and strings of caudal vertebrae. There is no evidence of preburial weathering or breakage, and trample scratch marks are rare. More than 20% of the bones exhibit irregular, mm-scale pits occur on the shafts and the articular ends of limb bones are commonly hollowed out. The irregular pits are termite foraging traces, and hollows indicate extensive mining by these insects. At least seven individuals of *Abydosaurus* are present, representing at least two ontogenetic stages (juveniles and subadults).

Together, these observations indicate the following: (1) the catastrophic death of a sauropod herd; (2) partial carcass maceration; (3) minor transportation, including articulated units (skulls, vertebrae, limbs); (4) rapid burial in migrating, ephemeral, branches of a distributary fluvial system; (5) channel migration resulting in *in-situ* scouring of the upper surface of some bones; (6) burial of scoured bones. Termite infestation occurred both prior to, and after, fluvial entrainment and burial.

Keywords: *Abydosaurus*, Naturita Formation, taphonomy, sedimentology, distributive fluvial system, Dinosaur National Monument, DNM-16

ACKNOWLEDGMENTS

The leaders, staff, and summer interns of the National Park Services' Dinosaur National Monument were crucial to this project. Special thanks are extended to monument paleontologist Dr. Daniel Chure for his help and permission to conduct research in Dinosaur National Monument. I thank Nicole Ortiz, Darby Holmes, Kevin Stuart, Haniff Souleiman, Kimberly Sowards, and Melissa Gonzalez for their assistance with field work, software, and graphics. Allan J. Matthews helped with photography and lab work. Drs. Ray Wilhite and Rod Scheetz's assistance with bone identification and paleontology expertise, and Drs. Tom Morris and Gary Weissmann's assistance in sedimentology principles is gratefully acknowledged. Drs. Scott Ritter and Sam Hudson provided invaluable advice, edits, and encouragement.

TABLE OF CONTENTS

LIST OF FIGURES AND TABLES

1 INTRODUCTION

In North America, Cretaceous sauropod dinosaurs are relatively uncommon, and worldwide, sauropod skulls are rare due to their delicate construction (Chure et al., 2010; Zaher et al., 2011). *Abydosaurus mcintoshi*, described by Chure et al. (2010) was the first complete sauropod skull (DINO 16488) described from the western hemisphere. It was recovered from Dinosaur National Monument Quarry 16 (hereafter DNM-16) along with three other skulls (DINO 17848, 17849, 39727), ranging from complete skulls to an isolated braincase, as well as a number of articulated limbs, vertebrae, and other post-cranial bones. It is important to understand the depositional environment and the taphonomic processes that led to preservation of these.

With the discovery of *Abydosaurus*, differing interpretations of the boundaries of the members of the Cedar Mountain have been proposed. The upper bounds of the Cedar Mountain Formation are not well understood in Dinosaur National Monument, leading to ambiguity as to the boundaries between the different members of the Cedar Mountain Formation and the overlying Naturita Formation. Proposed stratigraphic positions of DNM-16 range from the Ruby Ranch Member (Masters et al., 2004; Maxson, 2011), the Mussentuchit Member (Chure et al., 2010), and an unnamed "transitional facies" (Kirkland et al., 2016). Our study clarifies the stratigraphic position of the quarry at the base of the Naturita Formation (formerly the Mussentuchit Member of the Cedar Mountain Formation).

The nature of the depositional environment has also been a point of conflict. The quarry sandstone has been described as an anabranching channel intersection or deep scour (water hole) of an anastomosing fluvial system based on isolated channel morphology and rapid sedimentation rates from modern analogues in Cooper Creek, Australia and flume experiments (Masters et al., 2004; Maxson, 2011). However, given recent studies on distributive fluvial

systems (Fisher et al., 2007; Nichols and Fisher, 2007; Hartley et al., 2010; Weissmann et al., 2010; Nichols, 2012; Weissmann et al., 2013; Owen et al., 2015) and the information provided in our study, we propose the depositional environment more accurately aligns as a distributive fluvial system.

This study provides a background of the quarry and analyzes the sedimentology and taphonomy of the quarry with discussions and interpretations after each section, followed by the overall discussion and conclusion. With this, we seek to better constrain the depositional environment and stratigraphic position of the quarry and to understand the taphonomy of DNM-16.

1.1 Study Area

The primary emphasis of the study is the ~10 m^2 type locality of *Abydosaurus mcintoshi*, officially designated DNM-16 in National Park Service records. Quarry DNM-16 is about 260 m north of the Dinosaur Quarry Visitor Center and 400 m west of the Carnegie Quarry exhibit, within Dinosaur National Monument, Utah (Fig. 1). The quarry is located on the southwestern flank of the Split Mountain Anticline, a Laramide feature, where the beds dip some 62 degrees to the south (Silliphant et al., 2002). To put the quarry into stratigraphic context and to understand coeval depositional modes, the study area extends c. 150 m normal to strike and laterally about 1300 m along strike, with the quarry about 400 m east of the western boundary of the study area (Fig. 1B).

1.2 Age and Tectonic Setting

The Cedar Mountain and Naturita formations are fluvial-lacustrine deposits (e.g., Stokes, 1944; Young, 1960; Currie, 1998; Lorenz et al., 2006; Sprinkel et al., 2012; Carpenter, 2014). Two U-Pb radiometric ages have been recovered from detrital zircons from the Naturita

Formation, in or close to, the study area. Mudstones incised by the quarry sandstones yield a maximum depositional age of 104.46±0.95 (Chure et al., 2010) while a unit higher in the section gives a maximum depositional age of 101.4±0.4 Ma (Kirkland et al., 2011). Therefore, the local Naturita Formation can be no older than the late Albian—just below the Early and Late Cretaceous boundary using ages in Walker et al. (2012). In the late Albian, western Utah was subject to crustal loading from the Cordilleran thrust belt (DeCelles, 2004). One consequence of this loading was the creation of a backbulge. The Cedar Mountain Formation terrestrial sequence stratigraphy was pioneered by Currie (1997). We recognize the two sequences LK-1 and LK-2 from this area. However, we adopt the sequence boundaries of Greenhalgh and Britt (2007) and Sorensen (2011). The Morrison Formation and basal sequence (LK-1) of the Cedar Mountain (Buckhorn Conglomerate, Yellow Cat, and Poison Strip members, sensu Greenhalgh and Britt, 2007) are hypothesized to have been deposited east of the backbulge in central Utah (Currie, 1998). The other stratigraphic sequence (LK-2) of the Cedar Mountain Formation (the Ruby Ranch Member overlain by the Naturita Formation, sensu Sorenson, 2011) was later deposited as the foredeep basin overfilled and onlapped the forebulge in Currie's (1998) model.

1.3 Local Stratigraphy and Lithology

The Cedar Mountain Formation unconformably overlies the Morrison Formation (Currie, 1997, 1998; Greenhalgh, 2006; Hokanson, 2011; Sprinkel et al., 2012) with the hiatus spanning some 25 Ma (Eberth et al., 2005) (Fig. 2). The Cedar Mountain Formation, in turn, is overlain by the Naturita Formation, which consists primarily of overbank mudstones and sandy fluvial channels. The uppermost fluvial sandstones of the Naturita Formation are capped by the Mowry Shale (Walton, 1944). The focus of this study is Quarry DNM-16. The quarry is at the base of

an array of small, thin, poorly confined fluvial sandstone channels low in the Naturita Formation just above the Cedar Mountain Formation (Fig. 2).

1.3.1 Morrison Formation

The Brushy Basin Member is the uppermost unit of the Morrison Formation and is dominated by silty mudstones, many of which are pedogenically overprinted. The upper few meters of the Morrison Formation are typically marked by a thick, well-developed paleosol with root traces, slickensided peds, mottles, and iron stains (Stokes, 1944; Greenhalgh, 2006) interspersed with occasional sandstone-filled paleochannels. This member is interpreted to have been deposited in a low-sinuosity fluvial system that was altered by pedogenic and groundwater processes (Currie, 1998). The Morrison/Cedar Mountain Formation unconformity is described as a paleovalley resulting from the Cedar Mountain Formation fluvial systems eroding the top of the Morrison Formation (Currie, 1997, 1998; Greenhalgh, 2006; Hokanson, 2011; Sprinkel et al., 2012).

1.3.2 Cedar Mountain Formation in Dinosaur National Monument

The Cedar Mountain Formation was established to describe strata dominated by conglomerates, sandstones, and mudstones in the San Rafael uplift of Utah that are bounded below by the Morrison Formation and above by the Dakota Sandstone/Formation/Group and/or mudstones of the Cretaceous Interior Seaway (Stokes, 1952). Young (1960, 1965) renamed the sandstones and carbonaceous mudstones of the Dakota Sandstone/Group on the Colorado Plateau the Naturita Formation, because the relationship to the Dakota Sandstone type locality in Nebraska could not be confirmed. Kirkland, et al. (1997) redefined the Cedar Mountain Formation and divided it into an idealized layer-cake formation with the Buckhorn Conglomerate

and/or Yellow Cat Member at the base, overlain by the Ruby Ranch Member which in turn was overlain by the Mussentuchit Member in western extents of the formation.

Greenhalgh (2006) and Greenhalgh and Britt (2007) determined that the Yellow Cat Member, Poison Strip Sandstone, and Buckhorn Conglomerate are contemporaneous and represent different facies (floodplain, stream channel, and paleovalley fill, respectively) of the single terrestrial sequence (LK-1) at the base of the Cedar Mountain Formation.

The Ruby Ranch Member is characterized by non-smectitic clays that are often mauve with abundant caliche horizons that weather out as nodules (Kirkland et al., 1997). It contrasts with the Mussentuchit Member, which is characterized by smectitic mudstones and fewer caliche horizons. As defined by Kirkland et al. (1997) the Mussentuchit Member consists of the carbonaceous mudstones of the traditional Dakota Sandstone/Group—Young's (1960) Naturita Formation terminology was seldom used (Carpenter, 2014). The Mussentuchit Member, as defined, left the sandstones of the Dakota Sandstone as a separate formation consisting of sandstone beds and channels at varying positions within or on top of the Mussentuchit Member of the Cedar Mountain Formation. Sorensen (2011) determined that the Dakota Sandstone on the Colorado Plateau is fluvial in origin, with laterally extensive sandstones representing meander belts of rivers and the Mussentuchit Member of the Cedar Mountain Formation representing floodplain deposits of those rivers. In this paper, we use the term Naturita Formation, following Young (1960, 1965) and corroborated by Carpenter (2014), in including mudstones and related lithologies, as did Sorenson (2011), who considered the Mussentuchit Member of the Cedar Mountain Formation of the Kirkland et al. (1997) and "Dakota Sandstone" to be overbank and channel deposits, respectively, of the same terrestrial sequence (LK-2). To clarify, we use the term Naturita Formation for strata bounded below by the Ruby Ranch

Member of the Cedar Mountain Formation and above by reworked marine mudstones and sands of the Mowry Shale. Therefore, our model consists of the Morrison Formation, the Yellow Cat, and Ruby Ranch members of the Cedar Mountain Formation, followed by the Naturita Formation (Fig. 2).

2 METHODS

2.1 Sedimentology Methodology

We employed an outcrop-scale analysis of the DNM-16 Quarry and surrounding genetically-related beds in order to identify bedforms, grain size, composition, and morphology. Bedform paleocurrent and channel depth-to-width ratios were measured in order to constrain the type of environment in which the dinosaurs were deposited. The sand bodies themselves are poorly defined, the bounds of which are gradational into the surrounding mudstones or are poorly exposed. For this reason, we exclude the gradational and covered sections, and only include the recognizable sandstones as the primary channel bodies. Satellite and aerial imagery was used to analyze channel morphology and stratigraphic position. Additionally, three stratigraphic sections were measured from the upper reaches of the Morrison Formation up to the base of the Mowry Shale.

2.2 Taphonomy Methodology

Bones were excavated and prepared using traditional methods. This study utilized traditional methods as described by Britt et al. (2008; 2009) including a micro and macro examination of the bones using a light source raking across a bone's surface to accentuate marks, scratches, and other bone surface modifications. A database with bone information was linked to the quarry map utilizing MAPublisher for Adobe Illustrator to study bone orientation and association, the minimum number of individuals (MNI), taxon and element distributions, and

patterns of articulation and association. Methods will be described in more detail for each aspect in their respective sections.

3 STRATIGRAPHIC POSITION

Several stratigraphic positions have been determined for DNM-16 in previous work. We tested these conclusions by comparing the lithologies within, and immediately below, the quarry to definitions of the Ruby Ranch Member of the Cedar Mountain Formation and the mudstone facies of the Naturita Formation, and the unconformity between these stratigraphic units. Masters et al. (2004) and Maxson (2011) asserted the quarry is located within the Ruby Ranch Member of the Cedar Mountain Formation. It is unclear how they determined the position except for citing Kirkland et al. without citing the year. Presumably, they were referring to Kirkland et al. (1997), in which the Ruby Ranch Member is defined. Chure et al. (2010) concluded DNM-16 was near the base of the Mussentuchit Member of the Cedar Mountain Formation, which, in the terminology we adopt for this paper, would be the base of the Naturita Formation. Sprinkel et al. (2012) determined the quarry is in the Ruby Ranch Member of the Cedar Mountain Formation based on age (chronostratigraphy). In the most recent paper dealing with the stratigraphic position of DNM-16, Kirkland et al. (2016) placed it on the boundary of the "Ruby Ranch Member" facies (quotes are theirs) and the overlying "transitional" facies, where the "transitional" facies is similar to the Mussentuchit Member. Although the terminology differs, Kirkland et al. (2016) agrees with the stratigraphic position and lithology given in Chure et al. (2010).

Our analysis corroborates the position given in Chure et al. (2010) and followed by Kirkland et al. (2016), namely that the DNM-16 Quarry channels are at, or just above, the base of the Naturita Formation. Locally, the base of the Naturita Formation consists of white or light

grey smectitic mudstones or sandstones, none of which are overprinted with caliches. The top of the underlying Ruby Ranch Member of the Cedar Mountain Formation is marked by green, non-smectitic mudstone (Fig. 3). Below this diagnostic green mudstone, the channels are calcareous or overprinted with caliches, calcretes, and chert nodules that are diagnostic of the Ruby Ranch Member.

The varying proposed stratigraphic positions for DNM-16 may have arisen from the fact that the Naturita Formation channels are fluvial in nature and pinch and swell, and are so variable in the Dinosaur National Monument area. For this reason, we base our study on lithologic characteristics and conclude that DNM-16 is located at or near the base of the Naturita Formation based on the first occurrence of the presence of smectitic clays, a definitive character of that formation.

4 SEDIMENTOLOGY

To gain insights into the depositional environment of DNM-16, its sandstones and their intervening mudstones were systematically studied by (1) determining the gross morphology of sandstone bodies/channels and (2) by dividing the sandstones and mudstones into lithofacies and noting their interrelationships.

4.1 Channel morphology

4.1.1 Naturita Formation Channels

The Naturita Formation possesses an abundance of laterally accreted channels, indicating a low accommodation system (Currie, 1997) (Fig. 4A). These larger channels are similar to the bulk of the Naturita Formation ("Dakota Sandstone") channels, being meander belts/tracts (Sorenson, 2011). Meandering channels also have a low aspect ratio as described by Fisher et al. (2007), with well-defined bounds.

4.1.2 DNM-16 Channels

The extent of the quarry-related channel complex is relatively small, covering 230 m from east to west with an overall thickness of approximately 15 m. Within this channel complex, the individual sandstone lenses are thin (0.25–2 m thick) with widths that vary from a few to tens of meters. Their width-to-thickness aspect ratios range between 8:1 and 28:1, with an average ratio of 18:1. These sandstones are much smaller than the typically wide and thick channels (formerly termed the Dakota Sandstone) of most of the Naturita Formation.

The overall pattern within the quarry-related channel complex is isolated, thin sandstone lenses separated by sandy mudstones and mudstones, with an erosive to gradational basal contact to the mudstones. With the mudstones dominating the system, the overall cross-sectional morphology lacks channel amalgamation or lateral accretion within the channel complex (Fig. 4B). On the east side of the channel complex, the sandstones sweep up-section.

In the Ebro Basin, Nichols and Fisher (2007) recognized that many floodplain facies contained thin sand sheets deposited by unconfined flows. The poorly confined DNM-16 channels are similar to the Ebro Basin floodplain sheet sands. Fisher et al. (2007) classified channel types with their associated aspect ratio. In that classification, the DNM-16 channels' aspect ratios align as minor channels and sand sheets, demonstrating the DNM-16 channels are poorly confined (Fig. 5). The isolation of these poorly confined, fine-grained sandstone channels within mudstones, as opposed to amalgamated or laterally accreted sandy channels, indicate the bones were deposited in the distal reaches of a relatively high accommodation system in relation to the larger fluvial channels that are typically found higher in the Naturita Formation.

4.2 Lithofacies Descriptions

As described in 4.1, the DNM-16 channel complex is characterized by poorly defined, thin, curved, lensoidal sandstones bounded by silty mudstones. To better understand these sand and mudstone dominated packages, we subdivided each into lithofacies based on grain size, bedding, and sedimentary structures (Table 1).

4.2.1 Sandstone Lithofacies (S)

The sandstone lithofacies group is divided into eight lithofacies, all of which contain <25% silt, clay, and mud. All are poorly sorted and immature (Fig. 6). Excluding the bones and clay rip-up clasts, grain sizes range from very coarse to very fine. The dominant grain size is between medium and fine sand. Sand grains are angular to sub-angular quartz with a substantial amount of lithic grains. The sandstone lithofacies are further divided by bedding and sedimentary structures.

Massive Sandstone (Sm)

Lithofacies Sm is clean with medium and very fine sand, with a few beds of coarse to medium sand (Fig. 6C). It is massive and homogenous with occasional relict lamina/sedimentary structures. The massive structure is attributed to bioturbation of a sandstone that originally had sedimentary structures.

Planar-Laminated Sandstone (Sp)

The planar sandstones are composed of fine to very fine sand (Fig. 6A-C; Fig. 7C-D). They are planar-laminated and common in the quarry and related beds. Planar laminations are indicative of low velocity flow conditions or extremely high velocity flow conditions, however, due to high mud contents, we believe the former to be the dominant flow condition (Southard and Boguchwal, 1990).

Ripple-Laminated Sandstone (Sr)

This lithofacies primarily contains medium to fine grained sand (Fig. 6D; Fig. 7B). It also contains ripple laminations and resembles flaser bedding with dipping, laminated foresets. In three dimensions, the dipping foresets have linear and non-linear current ripples. In some lenses, where the mud content is slightly higher, the resemblance to flaser bedding is more pronounced. Alternating sand and mud laminations are typically attributed to bimodal flow conditions with tidal influence. However, flaser bedding is also a sign of ephemerality and is commonly associated with desiccation mud cracks in ephemeral streams (Bhattacharya 1997; Martin, 2000).

Climbing Ripple-Laminated Sandstone (Scr)

This common lithofacies contains medium to very fine grained sand (Fig. 6E). It is dominated by climbing ripples rather than planar or tabular bedding like the ripple-laminated sandstone (Sr) lithofacies. Flaser-like bedding is common. The abundance of this lithofacies points to a fast rate of sedimentation with a high sediment to fluid ratio or a rapid decrease in flow velocity (Ashley et al., 1982). Flaser-like bedding is recognized as a sign of ephemerality and is commonly associated with desiccation mud cracks in ephemeral streams (Bhattacharya 1997; Martin, 2000), which is the case here as there are no marine deposits connected to the DNM-16 channels.

Trough Cross Stratified Sandstone (St)

Lithofacies St is very coarse to fine grained (Fig. 6B; Fig. 7C). Only a few occurrences of this lithofacies are present around the DNM-16 channels. It is characterized by lenses and beds with large, low-angle cross-sets between 25- and 50-cm-thick. A 3D view of the cross-sets reveals trough shaped contacts in the dip direction of the cross-sets. Trough cross bedding is

indicative of rapid flow velocity, likely indicating the initial reactivation of the system (Southard and Boguchwal, 1990).

Undulatory Bedded Sandstone (Su)

Although very coarse to very fine sands are present in this facies, medium to fine fractions dominate (Fig. 6A and 6F). Mud content is highly variable, changing laterally within a single body and from sand body to sand body. The thin sandstones exhibit swaley-like bedding and are similar to oblique trough cross bedding and scour and fill structures. The undulatory bedding or scour and fill structures may denote rapid sedimentation, but they also denote variations in flow velocity and turbulence within the flow itself. This lithofacies may also be closely related to the trough cross stratified sandstone (St) lithofacies. The flow conditions belong to the upper flow regime and display rapid deposition with chaotic flows scouring and redepositing (Coleman and Gagliano, 1960; Southard and Boguchwal, 1990).

Rip-up Clast Filled Sandstone (Scl)

This lithofacies ranges from medium to very fine grains and contains grey, oblate clay clasts with diameters up to 30 mm (Fig. 6G). The clasts are most abundant beneath and adjacent to bones in the quarry. The clay rip-up clasts are similar to the grey clay mudstones indicating scouring from the underlying mudstone.

Convoluted Bedded Sandstone (Scb)

This sandstone is comprised of medium to very fine sand (Fig. 6H). The lamina in this lithofacies pinch and swell and in places resemble dish and pillar structures where laminations are disrupted via soft sediment deformation rather than primary deposition. The convoluted bedding is attributed to trapped fluids, which indicates the rate of sedimentation was more rapid

than the rate of dewatering, causing the bedding to look massive and to create wavy, pinching and swelling lamina (Lowe and LoPiccolo, 1974)

4.2.2 Heterolithic Lithofacies (H)

This lithofacies group is diagnosed by a clay content >25%, creating a heterolithic mix of interbedded sandstone and mudstone (Fig. 7). The quartz grains range from very coarse to very fine sand, with fine to very fine sands being the most abundant. The sands grains are poorly sorted and immature. These lithofacies are poorly cemented, friable, flakey, and fissile, with no visible evidence of bioturbation. They occur beneath and between the sheets and lenses of the sandstone lithofacies. They can also occur above and adjacent to the mudstone lithofacies. The exact nature of the heterolithic and mudstone lithofacies is not fully understood because they are easily eroded and often alluvium covered. For those reasons, bedforms in this facies group are difficult to identify. The heterolithic facies group are define primarily on bedforms**.**

Interbedded, Planar-Laminated Sandstones and Mudstones (Hp)

The planar-laminated sandstone of this facies is very immature and has a high mud content (Fig. 6B and 6D; Fig. 7A and 7C-D**)**. Individual units range from 2 mm to 20 mm thick. The interbedded mudstone laminations are generally between 2 mm and 10 mm thick. This lithofacies is common in the quarry and in some cases weathers with a globular popcorn texture due to smectitic clay (Fig. 7A). The planar laminations represent times of low flow velocity (Southard and Boguchwal, 1990).

Interbedded, Ripple-Laminated Sandstones and Mudstones (Hr)

The ripple-laminated sandstone is immature and has a high mud content with sand grains between coarse to very fine grained, with dominantly fine grained sand and relatively few isolated coarse grains (Fig. 6D; Fig. 7B). The sandstone thicknesses range from 2 mm to 20 mm

thick. The interbedded mudstone laminations are generally between 2 mm and 10 mm thick. They are distinguished by the shallow dipping foresets on a millimeter scale and produce a lenticular-like to wavy-like texture with the interbedded mudstone. The ripple laminations are indicative of high velocity flows relative to the other heterolithic facies (Southard and Boguchwal, 1990).

Interbedded, Trough Cross Bedded Sandstones and Mudstones (Ht)

There are only a couple instances of this lithofacies (Fig. 7C). The sandstone is very immature, has a high mud content, and though it is dominanted by fine to very fine sand, it ranges from very coarse to very fine sand. The thicknesses range from 2 mm to 20 mm thick. The interbedded mudstone laminations are generally between 2 mm and 5 mm thick. The dipping foresets terminate against the troughs of neighboring bedforms and the troughs have a sharp basal contact. The cross bedding is created in upper flow regime conditions (Southard and Boguchwal, 1990).

4.2.3 Mudstone Lithofacies (M)

We recognize two mudstone facies. They are composed primarily of mud, silt, clay, or a mixture with the grain size smaller than very fine sand. Mudstones are the dominant lithofacies in the DNM-16 area. Little sand is present. Smectitic clay is common in this lithofacies, evidence by the popcorn-like texture of exposures. The mudrocks are generally grey toned colors, with a tint of green in some cases. This lithofacies is subdivided based on physical characteristics.

Planar-Laminated Mudstone (Mp)

Lithofacies Mp has weak planar laminations, with low fissibility and a greenish, grey hue (Fig. 7E). The facies contains peds and gypsic snowballs (Buck and Van Hoesen, 2002; Buck et

al., 2010), and is apt to be highly smectitic. Buck and Van Hoesen (2002) and Buck et al. (2010) interpret the snowballs to represent an evaporative paleosol-forming environment and the peds indicate a soil horizon (Retallack, 2001). The grey indicates a poorly drained environment (Weissmann et al., 2013; Hartley et al., 2013); however, there are no definitive lacustrine or playa deposits, so the surrounding flood plain area may have been somewhat paludal. This lithofacies is either the very distal portion of the flow or the overbank deposits.

Homogenous Mudstone (Mn)

In this lithofacies, the mudstones are grey and tend to break into nodules without definite cleavage planes (Fig. 7F). It has little to no variation in color or composition throughout and has more of a green tint than the planar laminated mudstones (Mp). These mudstones have less smectite noted by the lack of surficial popcorn textures. This lithofacies may be the result of heavy bioturbation to the point where the burrows are unrecognizable. This lithofacies represents overbank deposits.

5 TAPHONOMY

The taphonomic study mainly focuses on the micro and macro observations, with macro scale dealing with the map analysis and the overall fossil assemblage and the micro scale dealing with the actual skeletal abrasions and surface markings.

5.1 Assemblage Characteristics

The DNM-16 Quarry map was compiled over several field seasons spanning over a decade, with c. 260 collected elements. The map is generally complete except that some of the first bones collected were not mapped. The map provides only a 2D plan view—the vertical positions of bones were not noted during collection. The paper field maps were digitized, with

each bone created as a distinct object. Each object was linked to a database in the GIS program, MAPublisher by Aveza Systems, to facilitate analysis.

5.1.1 Taxonomy

Only two species are known to occur in the DNM-16 Quarry, the brachiosaurid sauropod *Abydosaurus mcintoshi* and a small theropod, represented by a few small teeth. Decades ago, Robert Bakker collected parts (tibia, astragalus, dorsal vertebra, pedal phalanges and fragmentary femur) of a small coelurosaurid theropod from the channel complex that includes DNM-16. The exact site was not recorded but it is possible it came from what became DNM-16. The specimen is cataloged into the Museum of Comparative Zoology at Harvard as MCZ 2404. The MCZ theropod is not included in our study due to ambiguous site information, but is noted here as the specimen may have come from DNM-16. In sum, the quarry is overwhelmingly dominated by a single taxon, *Abydosaurus mcintoshi*, making it a monospecific, macrofossil assemblage following the definitions of Behrensmeyer (2007).

In a time-averaged death assemblage, we expect to find several different species, however this quarry is dominated by a single taxon, *Abydosaurus*, represented by multiple individuals, discussed in Section 5.1.3. This *Abydosaurus* assemblage provides strong evidence for a single catastrophic event as opposed to a time-averaged assemblage. If this is the case, it also indicates that *Abydosaurus mcintoshi* was likely gregarious, a habit that is unusual, but previously noted for some sauropods (see Myers and Fiorillo, 2009).

5.1.2 Element Distribution

Recovered bones are enumerated in Table 2 and their distribution is shown in Fig. 8. Collecting was biased against small bone fragments, which were usually not collected.

To test the assemblage for evidence of hydraulic sorting we divided the bones into modified Voorhies groups (Voorhies, 1969; Behrensmeyer, 1975). We modified the groups following Britt et al. (2009) because studies of sorting performed on modern bones (e.g., Voorhies, 1969; Behrensmeyer, 1975) may not accurately represent hydraulic impact on the large bones of sauropods. Articulated units were included in our shape classes based on the shape of the articulated unit, not the individual bones. The hydraulic fluid is also likely denser than 1.0 g/cc due to the increased sediment load, leading to rapid burial, which is discussed later. Densities are not included in these studies due to unknown pre-fossilized bone densities. Instead, we use a size classification based upon the maximum dimension of the recovered elements. The groups are labeled as:

Small: <= 199 mm

Medium: 200-499 mm

Large: >=500 mm

The size distribution shows a higher frequency of small elements. However, when combining the elements that are > 50 cm in maximum dimension, they have a frequency of 55, which shows there are numerous large elements. Articulated unit dimensions were summed and counted as one larger unit. The shape distribution shows an abundance of rod-shaped elements and relatively few block and complex elements. This may be caused by double counting rib fragments coupled with inclusion of flat and block elements into articulated units. The strings of vertebra alone would greatly increase the percentage of block elements if they were included as separate vertebra. The same is true for the skull elements and the complex shaped elements, which would better reflect the shape groups of an assemblage with no sorting bias. Overall, the

element distribution may have a slight sorting bias, but not enough to indicate substantial winnowing, sorting, or lag deposits described by Voorhies (1969) and Behrensmeyer (1975).

5.1.3 MNI

The minimum number of individuals (MNI) was determined using the femora, which are the most common element that could be identified as to sidedness. The left femora give an MNI of seven *Abydosaurus mcintoshi* individuals. The two theropod teeth provide a MNI of one for the theropod. Thus, at least eight individuals are represented in the quarry.

5.1.4 Ontogenetic Representation

There are two ontogenetic stages represented in the quarry for *Abydosaurus*. Like the MNI, we used the left femora to delineate the size range of the individuals (Fig. 9), with one that is slightly larger than the others (DINO 44912), and one that is significantly smaller than the others (DINO 44913). The smallest femur likely represents a juvenile, while the others belong to subadults, which is confirmed by growth ring analysis conducted on core plugs removed from the bones by Michael D'Emic (Michael D'Emic, Personal Communication, 2017). There are also two large vertebrae, 71.5 cm long (DINO 44914) that may pertain to an individual larger than represented by DINO 44912, the largest femur. These may represent a large subadult or a possible third adult stage, the largest individual in the quarry.

In a time-averaged assemblage, we expect to find a bimodal distribution in ontogenetic representation as the normal mortality of individuals is high for both juveniles and for older adults (Behrensmeyer, 2007). The majority of the *Abydosaurus* individuals at DNM-16 are subadults, suggesting a single catastrophic event killed off at least seven individuals, six of which were subadults—the strongest portion of the population, with the lowest probability of dying of non-catastrophic causes (Behrensmeyer, 2007).

5.1.5 Orientation

Bone orientation was measured using MAPublisher (Avenza, 2016), a module addition to Adobe Illustrator, by measuring the angle between 0° and 180° for orientation, and using 360° for vectors. Rose diagrams were plotted and analyzed using PAST (Hammer et al., 2001), plotting two-way directionality of the bones (n=90) and vectors with the larger or proximal end of the bone as the origin (Fig. 10). We measured orientations on disarticulated bones with a minimum of a 3:1 length-to-width ratio, following the recommendation of Voorhies (1969). Articulated units treated in the same manner. PAST uses Rao's U spacing test, which tests the hypothesis of uniformity around 360°, designed for circular data, meaning the p value will be one for perfectly isotropic orientations and zero if every measurement is perfectly unidirectional. We also use Rayleigh's test, which tests against a random bone orientation.

The individual bones and articulated units show a strong N-S trend. Rao's U test produces a p value of .06, which denotes a probable anisotropic orientation, but not conclusively. Rayleigh's test produced a p value much less than .01 and satisfies the assumption of unimodal distribution, meaning we can reject the null hypothesis and conclusively say that the orientations of the bones are not isotropic and there is a preferred orientation.

The sample size for disarticulated bones and articulated units with a large and small end we used to test for flow direction is small (n= 21) and this test did not yield statistically significant p values.

The bone orientations corroborate our bedform paleocurrent measurements (n=27) with flow directions to the north (Fig. 11). During the Cretaceous, the inundation of the North American continent initiated in the North, which supports our bone orientation measurements indicating the flow was toward the North. The anisotropically orientated bones were likely

influenced by a semi-unidirectional, semi-consistent flow as opposed to a single flooding event where the bones would be frozen or suspended in a chaotic, isotropic flow orientation (Eberth et al., 2006; Britt et al., 2009). We also see the articulated limbs in a straight orientation as opposed to bent at the joints, meaning the distal end of the limbs are oriented parallel to flow direction. This suggests a sustained flow that was sufficient to orient an entire articulated unit. We speculate that even brief, but rapid flow would be sufficient to orient bones and articulated units, such as limbs.

5.1.6 Articulation & Association

The quarry preserves articulated and closely associated portions of skeletons, but no fully articulated skeletons. Nineteen percent of the bones have at least two elements articulated while almost 33% of the bones are articulated or closely associated. The most notable articulation groups include the sauropod skulls, which, outside of the Late Jurassic, are exceptionally rare. In fact, the articulated skulls at DNM-16 were the first articulated sauropod skulls reported from the Cretaceous of the western hemisphere (Chure, et al., 2010). The most significant articulated specimens are the holotype skull articulated with four cervical vertebrae, DINO 16488, (Fig. 12A) and the rostrum of a damaged skull, DINO 17848, (Figs. 12B and 13A-C). The damaged skull preserves a completely articulated rostrum as well as partially disarticulated posterior portions of the mandible. In close association with these skulls are several disarticulated post-cranial elements. All the skulls are in the upper left quadrant of the quarry save for one isolated braincase, DINO 39727 (Fig. 12D).

Other articulated elements include several limb bones including the femora, tibiae, and fibulae (DINO 44913, DINO 44915, DINO 44916) (Fig. 12L-M and 12H) (Fig. 13D and 13F), articulated tibia and fibula (DINO 44922) (Figs. 12K and 13F), and one front limb including the

humerus, radius, ulna, and three metacarpals (DINO 44917) (Figs. 12N and 13E). Phalanges are uncommon and never found in articulation. There is also a partial foot with articulated metatarsals, which is closely associated to a tibia, fibula, and astragalus (DINO 44918, DINO 44916) (Fig. 12I and Fig. 13E). The remaining elements include an articulated sternal and coracoid (DINO 44919) (Fig. 12F), two cervical vertebrae (DINO 44914) (Fig. 12G), and partial pelvis with several sacral vertebrae with associated and articulated caudal vertebrae (DINO 16485) (Fig. 12E).

The articulated units were sheathed in at least minimal soft tissue, perhaps large amounts of tissue, while entrained in fluvial flow after minimal rotting, minimal transport, rapid burial (hyoid, and stapes bones, and sclerotic rings still in eye area of best skull), otherwise this level of articulation and preservation would not be probable.

5.2 Bone Modification

Bone modification reveals much about taphonomic factors impacting the bones (Voorhies, 1969; Shipman,1981; Behrensmeyer, 2007). Here, we present information on taphonomic features on the bones from DNM-16 and interpret these markings. Except for bones exposed to modern weathering or crushing/fracturing or due to tectonics, expansive clays, and slope slumping, most bones from DNM-16 provide substantial taphonomic information degradation.

5.2.1 Pitting

Approximately 20% of the bones bear some degree of pitting. This pitting ranges from clusters of numerous pits that are evenly and widely distributed across a bone's surfaces, to distinct isolated clusters of shallow pitting (Fig. 14). The pitting is either widespread across the entire bone or isolated to one or two surfaces, with 39% preferentially on the stratigraphic down side and 25% on all sides. We did not observe any isolated pits.

The individual pits are low in relief (<1 mm) with rounded edges. The pits are circular to elliptical with the outermost surface of bone being removed, but never breaching past the dense cortical bone. Several pits penetrate to 1.5-2 mm deep, however, these deeper pits are gradational as the edges merge with shallower pitting before they grade to deeper pitting. The dimensions of these pits are hard to constrain as the pits are never isolated. The edges are poorly defined and often coalesce with surrounding pits to form one large harvested surface. The pits still contain cemented matrix, which would not exist if the markings were modern in origin.

The ends of 6% of the limb bones are completely missing and often the ends of these bones not only lack articular surfaces but are occupied by concavities that extend deep into the bone shafts (Fig. 14A).

Dangerfield et al. (2005) and Britt et al. (2008) identified similar pitting patterns on fossil and modern bones. The pits on modern bones were created by termites (Wood, 1976; Wylie et al., 1987; Tappen, 1994; Backwell et al., 2012). These works noted that deep excavations into the ends of bones were the function of preferential insect scavenging of the softer, soft tissue-rich bone.

5.2.2 Scratch/Tooth Marks

Scratch marks are present on a single bone, DINO 44921, a scapula. The marks consist of cm-scale, similarly oriented, arcuate scratch marks c. 25 mm long and <1 mm deep (Fig. 14F). Aside from these, there are no definite scratch or damage marks caused post mortem.

These scratches are similar to trample marks from the Dalton Wells Quarry (Britt at al., 2009), however, the trample marks from Dalton Wells are very closely spaced with only a millimeter or two separating each mark in their sets, whereas these DNM-16 marks have c. 25 mm between each mark. In addition, trample marks are not visible on any other bones and due

to the high likelihood of flesh being present on the bones at the time of burial, they more closely related to tooth marks as a byproduct of vertebrate scavenging.

5.2.3 Pre-lithification Breakage

The fractures and breakage surfaces of the bones are rough, and perpendicular to the long axis of the bones. Pre-lithified breakage typically displays smooth, oblique fractures, if the bones are still fresh, or step fractures if the bones are dry (Shipman, 1981; Villa and Mahieu, 1991). The surfaces of the bones, although highly fractured, do not display any examples of pre-lithification breakage. Thus, there is no evidence of trampling in the quarry.

5.2.4 Weathering

Pre-burial weathering was noted following Behrensmeyer (1978). There is no evidence of weathering, indicating the bones were buried soon after death, before the bones could be weathered.

5.2.5 Abrasion

Except for a pair of large, articulated cervical vertebrae (DINO 44914), there is no evidence of abrasion. The neural arches and the upper portion of these cervical vertebrae are missing and they were not damaged or lost during collection. The uppermost preserved surfaces of both vertebrae are planar, with the upper surfaces in the same plane in the quarry. This plane was covered with mudstone at the time of discovery. Beneath the mudstone, the fine, internal trabeculae of the highly pneumatic vertebrae are visible (Fig. 13E).

This abrasion is interpreted as erosion by scouring. The bones were buried upright and scoured by a later, sand-laden flow through the same channel, which excised and smoothed the surface. During the waning flow mud settled over the abraded surface. It is possible that similar

scouring destroyed some bones. This suggests there may have been several episodes of burial, scouring, and secondary burial, and is strong evidence for the ephemerality of the system.

5.2.6 Crushing

We did not quantify the number crushed bones but crushing and other post-burial deformation is evident on many bones. The complete, articulated skull (DINO 16488) is moderately crushed about 50% from side-to-side and about 33% obliquely. Likewise, the two large cervical vertebrae are severely dorsoventally crushed, with an estimated 50% reduction in volume. More robust elements, such as limb bones and phalanges range from uncrushed to flattened. Crushing is attribute to post-depositional compaction of sediments. The relationship of the amount of crushing as related to sediment type (e.g., mudstone, to clayey sandstone, to clean sandstone) was not noted during collection or preparation. However, our experience in the lab with many vertebrate localities indicates crushing is largely tied to the amount of clay in the matrix. Clean sands minimize crushing while the greater the clay content, the greater is the amount of crushing. We conclude that variable clay content of the matrix at DNM-16 explains the variable degrees of bone crushing.

5.2.7 Post-Depositional Breakage

The fracture surfaces are rough, and propagate straight across the short axis of the bones as opposed to smooth and oblique. Micro fractures that do not propagate all the way through the bone are common. The straight fractures perpendicular to the long axis imply post-burial breakage (Shipman, 1981). All portions of broken bones are present which is symptomatic of *in situ* breakage and cementation, or cementation prior to breakage.

DISCUSSION

The stratigraphic, sedimentological, and taphonomic data presented above was conducted to provide new insights into the stratigraphic position, depositional environment, and development of the DNM-16 bonebed. In this section we consider the implications of these data.

The Ruby Ranch Member of the Cedar Mountain Formation is characterized by red, mauve, and purple paleosols (Kirkland et al., 1997) indicating an oxidized, well-drained, semiarid environment (Hartley et al., 2013). The top of the Ruby Ranch Member is commonly overprinted by a thick, highly oxidized paleosol (Sorensen, 2011), marking a depositional hiatus that we identify as the K2 sequence boundary. This paleosol is not present in the study area and it was likely eroded with development of the Naturita Formation system tract. The Naturita Formation is dominated by grey paleosols indicating poorly oxidized, poorly drained soils in a time when the climate was becoming more humid due to the encroaching seaway (White, et al., 2000), with the grey paleosols reflecting the shift to poorly drained conditions (Hartley et al., 2013). This marked change from well drained to poorly drained, coupled with the mud-dominated base of the Naturita Formation with sparse channels, shows a shift to relatively higher accommodation. Higher in the Naturita Formation, the channels laterally accreted in a low-accommodation system dominated by medium-sized rivers meandering across the landscape (Sorenson, 2011). Currie (1997), Greenhalgh and Britt (2007), and Sorensen (2011) identify a terrestrial sequence boundary at the top of the Ruby Ranch Member of the Cedar Mountain Formation (LK-2); however, they do not identify the system tract of the Naturita Formation (Mussentuchit/Dakota members in their papers). We believe the quarry to be located in a transitional to aggradational systems tract (Currie, 1997) as a non-marine, fluvial system.

Our sedimentological study focused on the channel complex that includes the DNM-16 quarry. Masters et al. (2004) and Maxson (2011) concluded that the DNM-16 channel complex

was created in an anastomosing fluvial system. Anastomosing fluvial systems have well defined channels and confined flows (Schumm, 1968; Miall, 1977). This is also the case for meandering fluvial systems, although they generally contain a single channel as opposed to branching channels (Allen, 1970). The channel morphology and lateral discontinuity of the DNM-16 sandstone channels do not fit a well-confined channel model. A braided fluvial system aligns with the rapid sedimentation, however this also does not match the stacking pattern, nor does it account for the abundance of mud and fine-grained sand in the DNM-16 system, as braided fluvial systems are generally sandy (Miall, 1977). We conclude the DNM-16 depositional environment was that of a distributive fluvial system, which diverts away from a primary channel and does not return. Distributive fluvial systems differ from tributary fluvial systems in that they are unconfined unless the channel is incising, channel dimensions decrease or remain constant distally in the system while tributary fluvial systems increase in dimensions, and grainsize decreases downstream with no input from tributaries (Davidson et al., 2013).

The repetitive vertical stacking of muds/fine sand deposition (lithofacies Sr, Sp, Hr, and Hp) alternated with medium sand deposition (lithofacies St and Su) is indicative of alternating low velocity and high velocity flow (Southard and Boguchwal, 1990). This is also evident from the abrasion of the two vertebrae that had the neural arches scoured off as the system reactivated after a time of little or no flow. Overall, the variance shows this to be a system that is ephemeral with times of high flow velocity, low flow velocity, stagnant flow, or no flow. The strongest evidence fluctuating flow is the flaser-like bedding (Bhattacharya 1997; Martin, 2000).

With the alternating lithofacies, the DNM-16 channels and surrounding area have abundant fine-grained material and mud. This is further punctuated by the lack of anything larger than very coarse sand, aside from the bones and gastroliths. We attribute this is due to the

ephemerality of the system. If flow was consistent the sediments would be better sorted and the muds winnowed out (Voorhies, 1969; Allen, 1970), but the local system is laden with fine-grained sediments, especially clays. In the Mississippi River, the bedload is primarily sand, while the suspended load is silt and clay. The silts and clays are transported through a consistent flow and are deposited in the Mississippi Delta (Lane, 1938). In the DNM-16 system, the mud and silt is not transported further, but is being deposited, indicating a waning flow. This supports our hypothesis that DNM-16 represents the distal reaches of a distributive fluvial system.

At the eastern edge of the DNM-16 channel system the terminal edges of sandstones curve upsection (Fig 4B). The bases of these sandstone channels are incised into floodplain mudstones, indicating channel scour, which is known to occur, even in the distal reaches of distributary systems (Weissmann et al., 2015), although the distal end of a system is typically not highly erosive. We speculate the upcurved ends of channels relates to it being a paleovalley fill and differential compaction of underlying floodplain clays.

In the distal portion of a distributive fluvial system, the sedimentation rate is high as the channels become less confined and the flow capacity decreases, which provides a mechanism for the bones to be rapidly buried. The abundance of climbing ripples in the quarry and related channels are indicative of rapid sedimentation rates. The articulation of the bones, due to the presence of soft tissue at the time of final burial, also indicates a rapid sedimentation rate. The absence of bone weathering indicates the bones were buried shortly after death. Behrensmeyer (1978), studied the weathering stages of bones in different environments over time. After one year of being exposed, every environment produced at least stage one weathering with a stage 3 from the swamp. Similarly, from the observation of modern, fresh carcasses, Voorhies (1969) discerns that after a year, the bones were cracked and split, showing signs of heavy weathering.

He also observed that bioerosion from insects and larger scavengers removed the flesh of a calf in two weeks and disarticulation was complete after almost three months. *Abydosaurus* is much larger than a calf and would have taken longer to strip the flesh and disarticulate. In either case, *Abydosaurus* was only partially disarticulated with no weathering. We suspect this means *Abydosaurus* was buried due to rapid sedimentation rates within weeks post mortem.

The presence of theropod teeth in the quarry as well as the possible tooth marks are evidence of possible vertebrate scavenging. With the abundance of *Abydosaurus* carrion, feeding would have been minimal and not aggressive, as was the case when a large number of elephants died during a drought (Coe, 1978). Voorhies (1969) states that if food were scarce or the bones were exposed for lengthy periods, they might have been devoured completely, however, if they are only exposed briefly, then the scavengers would have a short time to be selective before they were buried, meaning vertebrate scavenging occurred without abundant damage to the bones.

The selective feeding principle also applies to the maker of the only other feeding traces on the bones, termites. Termites probe to find the most nutrient-laden portions of bones - the cartilage-covered articular ends (Britt et al., 2008). In time, they would devour the entire bone if it were exposed at the surface or just below the surface (Wylie et al., 1987). Termite scavenging is expected to be the most abundant on the underside of the bones and on the articular ends where the insects are not exposed (Tappen, 1994). This is true in most of the bones, however, there are some that are pitted on all sides, providing two scenarios for the DNM-16 termite trace. In the first scenario, the bones are completely buried and the insects burrow on all sides of the bones without being exposed at the surface. In the second scenario, the bones were exposed long enough to exhibit burrowing on all sides. The former is more likely for two reasons. The bones

show no weathering, meaning they were not exposed at the surface for long, and even if the bones were exposed, they would be noticeably more pitted on the underside, which contradicts the even pitting seen on the bones. However, this may also be due to the presence of soft tissue, apart from the fact that bone DINO 44913 is the only articulated bone that exhibits noticeable pitting on the surface, which is only light pitting.

Masters et al. (2004) proposed the carcasses accumulated on sand bars between bifurcating channels, or sediment traps. Our finding that the assemblage is catastrophic and monospecific makes this an unlikely scenario because a perennial stream would likely trap carcasses of a variety of taxa.

In sum, the fluvial system of the DNM-16 channel complex is best explained by the distributive fluvial system hypothesis. The DNM-16 architectural and lithofacies elements, as well as the taphonomic conditions (Fig. 15), match the architectural and facies elements described by Fisher et al. (2007), Nichols and Fisher (2007), Nichols (2012), and Weissmann et al. (2013) (Fig. 16). The distributive fluvial systems also cover much of the earth today and are likely to be much more prevalent in the rock record than is currently recognized (Hartley et al., 2010; Weissmann et al., 2010). Finally, many of the fluvial systems are distributive fluvial systems in both the Cedar Mountain and Morrison formations, just below the Naturita Formation (Gary Weissmann, personal communication, 2016; Owen et al., 2015).

CONCLUSION

Abydosaurus was gregarious and the individuals preserved at DNM-16 died in a single catastrophic event during the late Albian middle Cretaceous as the Cretaceous seaway advanced southward. There was a marked changed of environment from the semiarid environment of the Ruby Ranch Member. The animals were preserved during a shift from an erosional phase to a

depositional phase at the base of the Naturita Formation, immediately above the Ruby Ranch Member of the Cedar Mountain Formation. The erosive nature of the Naturita and DNM-16 channels compiled with deep paleosols of the Ruby Ranch Member indicate a hiatus in deposition, which indicates the LK-2 sequence boundary at the base of the Naturita Formation.

The Naturita Formation consist overwhelmingly of smectitic clays. The base of the formation is mud-dominated with sparse channels, indicating high accommodation. Up-section, the accommodation space decreases, preserving conglomeratic to sandy horizons representing fluvial meander belts, which were subsequently flooded by the Mowry and Mancos seaway.

The DNM-16 system is an ephemeral distributive fluvial system with a high variance in flow velocity, grain size, mud content, and an abundance of angular grains and lithics. The sedimentation rate was high and this is likely due to a rapid decrease in flow velocity as the channels become unconfined or less confined leading to rapid burial of *Abydosaurus*. As the flow become unconfined, the flow ceased to scour and deposited sheet sands, or poorly channelized, minor channels. The high mud content indicates the quarry is located in the distal portions of the distributive fluvial system.

The quarry preserves a group of at least seven individuals, mainly subadult in age, with one juvenile and one possible adult or large subadult. The quarry is monospecific, which points to a single, localized event as opposed to a death assemblage over time. The carcasses were transported a short distance, with portions of skeletons held together with soft tissues. The bones were scavenged by small theropods before burial and by termites before and after burial. After burial, compaction of the muddy layers and local tectonics flattened, crushed, and fractured the bones.

This study clarifies the local stratigraphy, which has previously been a point of conflict. It also shows the DNM-16 depositional environment, previously interpreted as an anastomosing system, was a distributive fluvial system. Distributive fluvial systems are widespread across our planet, yet are given little recognition in the rock record. We hope this study will bring attention to their abundance in the rock record, solidify the stratigraphic nomenclature for the Dinosaur National Monument area, and bring to light the importance of incorporating taphonomic information into depositional environment interpretations.

REFERENCES

Allen, J.R.L., 1970, Studies in fluviatile sedimentation: a comparison of fining-upwards cyclothems, with special references to coarse-member composition and interpretation: Journal of Sedimentary Research, v. 40, n. 1, pp. 298–323

Ashley, G.M., Southard, J.B., Boothroyd, J.D., 1982, Deposition of climbing-ripple beds: a flume simulation: Sedimentology, v. 29, n. 1, pp. 67–79.

Avenza Systems Inc, 2016, MAPublisher: Version 9.9 for Adobe Illustrator. http://www.avenza.com/mapublisher

Backwell, L.R., Parkinson, A.H., Roberts, E.M., d'Errico, F. and Huchet, J.B., 2012, Criteria for identifying bone modification by termites in the fossil record: Palaeogeography, Palaeoclimatology, Palaeoecology, 337, pp.72–87.

Bhattacharya, A., 1997, On the origin of non-tidal flaser bedding in point bar deposits of the River Ajay, Bihar and West Bengal, NE India: Sedimentology, v. 44 n. 6, pp. 973–975.

Behrensmeyer, A.K., 1975, The taphonomy and paleoecology of Plio-Pleistocene vertebrate assemblages east of Lake Rudolf, Kenya: Bulletin of the Museum of Comparative Zoology v.146, pp. 474–578.

Behrensmeyer, A.K., 1978, Taphonomic and ecologic information from bone weathering: Paleobiology, v. 4, n. 2, pp. 150–162.

Behrensmeyer, A.K., 2007, Bonebeds through Time, in Rogers, R.R., Eberth, D.A., and Fiorillo, A.R., eds., Bonebeds Genesis Analysis, and Paleobiological Significance: Chicago, Illinois, and London, U.K., University of Chicago Press, pp. 65–101.

Britt, B.B., Eberth, D.A., Scheetz, R.D., Greenhalgh, B.W., and Stadtman, K.L., 2009, Taphonomy of debris-flow hosted dinosaur bonebeds at Dalton Wells, Utah (Lower Cretaceous, Cedar Mountain Formation, USA): Palaeogeography, Palaeoclimatology, Palaeoecology, v. 280, pp. 1–22.

Britt, B.B., Scheetz, R.D., Dangerfield, A., 2008, A suite of dermestid beetle traces on dinosaur bone from the Upper Jurassic Morrison Formation, Wyoming, USA. Ichnos, v. 15, pp. 59–71. DOI:10.1080/10420940701193284

Buck, B.J., and Van Hoesen, J., 2002, Snowball morphology and SEM analysis of pedogenic gypsum, southern New Mexico, USA: Journal of Arid Environments, v. 51, pp. 469–487.

Buck, B.J., Lawton, T.F., and Brock, A.L., 2010, Evaporitic paleosols in continental strata of the Carroza Formation, La Popa Basin, Mexico: Record of Paleogene climate and salt tectonics: GSA Bulletin, v. 122, no. 7/8, pp. 1011–1026.

Carpenter, K., 2014, Where the sea meets the land—the unresolved Dakota problem in Utah. In MacLean, J.S., Biek, R.F., and Huntoon, J.E., editors, Geology of Utah's Far South: Utah Geological Association Publication 43, pp. 357–372.

Chure, D., Britt, B.B., Whitlock, J.A., Wilson, J.A., 2010, First complete sauropod dinosaur skull from the Cretaceous of the Americas. Naturwissenschaften, v. 97, pp. 379–391. DOI 10.1007/s00114-010-0650-6.

Coe, M., 1978. The decomposition of elephant carcasses in the Tsavo (East) National Park, Kenya. Journal of Arid Environments 1, 71–86.

Coleman, J.M. and Gagliano, S.M., 1960, Sedimentary structures: Mississippi River deltaic plain: SEPM, Primary Sedimentary Structures, special publication v. 12, pp. 133–148.

Currie, B.S., 1997, Sequence stratigraphy of nonmarine Jurassic-Cretaceous rocks, central Cordilleran fore-land-basin system: Geological Society of America Bulletin, v. 109, no. 9, pp. 1206–1222.

Currie, B.S., 1998, Upper Jurassic–Lower Cretaceous Morrison and Cedar Mountain Formations, NE Utah–NW Colorado: relationships between nonmarine de-position and early Cordilleran foreland basin development: Journal of Sedimentary Research, v. 68, no. 4, pp. 632–652.

Dangerfield, A., Britt, B.B., Scheetz, R., and Pickard, M., 2005, Jurassic dinosaurs and insects: the paleoecological role of termites as carrion feeders: Geological Society of America Abstracts with Programs, v. 37, n. 7, pp. 443.

Davidson, S.K., Hartley, AJ., Weissmann, G.S., Nichols, G.J. and Scuderi, L.A., 2013, Geomorphic elements on modern distributive fluvial systems: Geomorphology, v. 180, pp. 82–95.

DeCelles, P.G., 2004, Late Jurassic to Eocene evolution of the Cordilleran thrust belt and foreland basin system, Western U.S.A.: American Journal of Science, v. 304, pp. 105–168.

Eberth, D.A., Brooks, B.B., Scheetz, R., Stadtman, K.L., and Brinkman, D.B., 2006, Dalton Wells: Geology and significance of debris-flow-hosted dinosaur bonebeds in the Cedar Mountain Formation (Lower Cretaceous) of eastern Utah, USA: Palaeogeography, Palaeoclimatology, Palaeoecology, v. 236, pp. 217–245.

Fisher, J.A., Nichols, G.J., Waltham, D.A., 2007, Unconfined flow deposits in distal sectors of fluvial distributary systems: Examples from the Miocene Luna and Huesca Systems, northern Spain: Sedimentary Geology, v. 195, n. 1–2, pp. 55–73.

Greenhalgh, B.W., 2006, A stratigraphic and geochronologic analysis of the Morrison Formation/Cedar Mountain Formation boundary, Utah: [MS: Brigham Young University, 61 p.

Greenhalgh, B., and Britt, B.B., 2007, Stratigraphy and sedimentology of the Morrison/Cedar Mountain formational boundary, east-central Utah. In, Willis, G.C., Hylland, M.D., Clark, D.L., and Chidsey, T.C., Jr., editors, Central Utah—diverse geology of a dynamic landscape. Utah Geological Association Publication 36, pp. 81–100.

Hammer, Ř., Harper, D.A.T., Ryan, P.D., 2001, PAST: Paleontological statistics software package for education and data analysis: Palaeontologia Electronica v. 4, n. 1, p. 9 http://palaeo-electronica.org/2001_1/past/issue1_01.htm

Hartley, A.J., Weissmann, G.S., Bhattacharayya, P., Nichols, G.J., Scuderi, L.A., Davidson, S.K., Leleu, S., Chakraborty, T., Ghosh, P., and Mather, A.E., 2013, Soil development on modern distributive fluvial systems: preliminary observations with implications for interpretation of paleosols in the rock record: New Frontiers in Paleopedology and Terrestrial Paleoclimatology: SEPM, Special Publication, v. 104, pp. 149–158.

Hokanson, W.H., 2011, Identifying complex fluvial sandstone reservoirs using core, well log and 3D seismic data—Cretaceous Cedar Mountain and Dakota Formations, southern Uinta Basin, Utah: [MS: Brigham Young University, 75 p.

Kirkland, J.I., Britt, B., Burge, D., Carpenter, K., Cifelli, R., DeCourten, F., Eaton, J., Hasiotis, S., and Lawton, T., 1997, Lower to Middle Cretaceous dinosaur faunas of the Central Colorado Plateau: a key to understanding 35 million years of tectonics, sedimentology, evolution, and biogeography, Brigham Young University Geology Studies, v. 42, pp. 69–103.

Kirkland, J.I., Madsen, S.K., Hunt, G.J., Waanders, G., Sprinkel, D.A., and O'Sullivan, P.B., 2011, Contacts, ages, and correlation of Lower Cretaceous strata on the north side of the Uinta Basin, northeastern Utah: Geological Society of America Abstracts with programs, v. 43, no. 4, p. 2.

Kirkland, J.I., Suarez, M., Suarez, C., Hunt-Foster, R., 2016, The Lower Cretaceous in east-central Utah—The Cedar Mountain Formation and its bounding strata: Geology of the Intermountain West, v. 3, pp. 101–228.

Lane, E., 1938, Notes on the formation of sand: Eos, Transactions American Geophysical Union, v. 19, n. 1, pp. 505–508.

Lorenz, J.C., Cooper, S.P. and Olsson, W.A., 2006, Natural fracture distributions in sinuous, channel-fill sandstones of the Cedar Mountain Formation, Utah: AAPG bulletin, v. 90, n. 9, pp. 1293–1308.

Lowe, D.R., and LoPiccolo, R.D., 1974, The characteristics and origins of dish and pillar structures: Journal of sedimentary petrology, v. 44, n. 2, pp. 484–501.

Martin, A.J., 2000, Flaser and wavy bedding in ephemeral streams: a modern and an ancient example: Sedimentary Geology, v. 136, n. 1, pp. 1–5.

Masters, S.L., Maxson, J.A., and Madsen, S.K., 2004, Anastomosing fluvial system of the Cedar Mountain Formation, eastern Utah—a paleoenvironmental and taphonomic analysis [abs.]: Geological Society of *America* Abstracts with Programs, v. 36, no. 5, pp. 60.

Maxson, J., 2011, Complex interactions between fluvial channels and syn-depositional pedogenic carbonate in the lower Cretaceous Cedar Mountain Formation and Dinosaur National Monument, Utah and Colorado [abs.]: Geological Society of America, Abstracts with Programs, v. 43, no. 4, pp. 2.

Miall, A.D., 1977, A review of the braided-river depositional environment: Earth-Science Reviews, v. 13, n. 1, pp. 1–62.

Myers, T.S., and Fiorillo, A.R., 2009, Evidence for gregarious behavior and age segregation in sauropod dinosaurs. Palaeogeography, Palaeoclimatology, Palaeoecology, v. 274, n. 1–2, pp. 96-104.

Nichols, G.J., 2012, Structural controls on fluvial distributary systems—the Luna system, northern Spain: SEPM, Recent Developments in Fluvial Sedimentology (SP39), pp. 269–277.

Nichols, G.J. and Fisher, J.A., 2007, Processes, facies and architecture of fluvial distributary system deposits: Sedimentary Geology, v. 195, n. 1-2, pp. 75–90.

Owen, A., Nichols, G.J., Hartley, A.J., Weissman, G.S., 2015, Vertical trends within the prograding Salt Wash distributive fluvial system, SW United States: Basin Research, pp. 1-17. DOI: 10.1111/bre.12165.

Retallack, G.J., 2001. Soils of the past. 2nd ed. Blackwell, Oxford University Press. 404 p.

Shipman, P., 1981, Life History of a Fossil: An Introduction to Taphonomy and Paleoecology, Harvard University Press, Cambridge, 222 p.

Schumm, S.A., 1968, Speculations concerning paleohydrologic controls of terrestrial sedimentation: Geologic Society of America Bulletin, v. 79, n. 11, pp. 1573–1588.

Silliphant, L.J., Engelder, T., and Gross, M.R., 2002, The state of stress in the limb of the Split Mountain anticline, Utah: constraints placed by transected joints: Journal of Structural Geology, v. 24, pp. 155–172.

Sorensen, A.E.M., 2011, Geologic mapping of exhumed, mid-Cretaceous paleochannel complexes near Castle Dale, Emery County, Utah: On the correlative relationship between the Dakota Sandstone and the Mussentuchit Member of the Cedar Mountain Formation. [MS: Brigham Young University, 61 p.

Southard, J.B. and Boguchwal, L.A., 1990, Bed configurations in steady unidirectional water flows: Journal of Sedimentary Petrology, v. 60, n. 5, pp. 658–679.

Sprinkel, D.A., Madsen, S.K., Kirkland, J.I., Waanders, G.L., and Hunt, G.J., 2012, Cedar Mountain and Dakota Formations around Dinosaur National Monument—evidence of the first incursion of the Cretaceous Western Interior Seaway into Utah: Utah Geological Survey Special Study 143, pp. 21, 6 appendices.

Stokes, W.L., 1944, Morrison Formation and related deposits in and adjacent to the Colorado Plateau: Geological Society of America Bulletin, v. 55, pp. 951–992.

Stokes, W.L., 1952, Lower Cretaceous in Colorado Plateau: AAPG Bulletin, v. 36, n. 9, pp.1766–1776.

Tappen, M., 1994, Bone weathering in the tropical rain forest: Journal of Archaeological Science, v. 21, n. 5, pp. 667–673.

Villa, P. and Mahieu, E., 1991, Breakage patterns of human long bones: Journal of Human Evolution, v. 21, pp. 27–48.

Voorhies, M., 1969, Taphonomy and population dynamics of an Early Pliocene vertebrate fauna, Knox County, Nebraska. University of Wyoming Contributions to Geology, Special Paper No 1, pp. 1–69.

Walker, J.D., Geissman, J.W., Bowring, S.A., and Babcock, L.E., compilers, 2012, Geologic Time Scale v. 4.0: Geological Society of America.

Walton, P.T., 1944, Geology of the Cretaceous of the Uinta Basin, Utah: Geological Society of America Bulletin, v. 55, n. 1, pp. 91–130.

Weissmann, G.S., Hartley, A.J., Scuderi, L.A., Nichols, G.J., Davidson, S.K., Owen, A., Atchley, S.C., Bhattacharyya, P., Chakraborty, T., Ghosh, P., Nordt, L.C., Michel, L., Tabor, N.J., 2013, Prograding distributive fluvial systems: geomorphic models and ancient examples: New Frontiers in Paleopedology and Terrestrial Paleoclimatology: SEPM, Special Publication v. 104, pp. 131–147.

Weissmann, G.S., Hartley, A.J., Scuderi, L.A., Nichols, G.J., Owen, A., Wright, S., Felicia, A.L., Holland, F., Anaya, F.M.L., 2015, Fluvial geomorphic elements in modern sedimentary basins and their potential preservation in the rock record: A review: Geomorphology v. 250, pp. 187–219.

White, T., Gonzalez, L., Ludvigson, G., and Poulsen, C., 2000, Middle Cretaceous greenhouse hydrologic cycle of North America: Geology v. 29, no. 4, pp. 363–366.

Wood, W. B., 1976, The skeletal material from the Brooloo Range and Rocky Hole Creek burial sites: Archaeology and Physical Anthropology in Oceania, v. 11, n. 3, pp. 175–185.

Wylie, F.R., Walsh, G.L., and Yule, R.A., 1987, Insect damage to aboriginal relics at burial and rock-art sites near Carnarvon in Central Queensland: Austral Entomology, v. 26, n. 4, pp. 335–345

Young, R.G., 1960, Dakota Group of Colorado Plateau: Bulletin of the American Association of Petroleum Geologists, v. 44, no. 2, pp. 156–194.

Young, R.G., 1965, Type Section of Naturita Formation: Geological Notes: AAPG Bulletin, v. 49, n. 9, pp. 1512–1516.

Zaher, H., Pol, D., Carvalho, A.B., Nascimento, P.M., Riccomini, C., Larson, P., Juarez-Valieri, R., Pires-Domingues, R., da Silva Jr, N.J., de Almeida Campos, D., 2011, A complete skull of an Early Cretaceous sauropod and the evolution of advanced titanosaurians: PLoS One, v. 6, n. 2, pp. e16663.

FIGURES

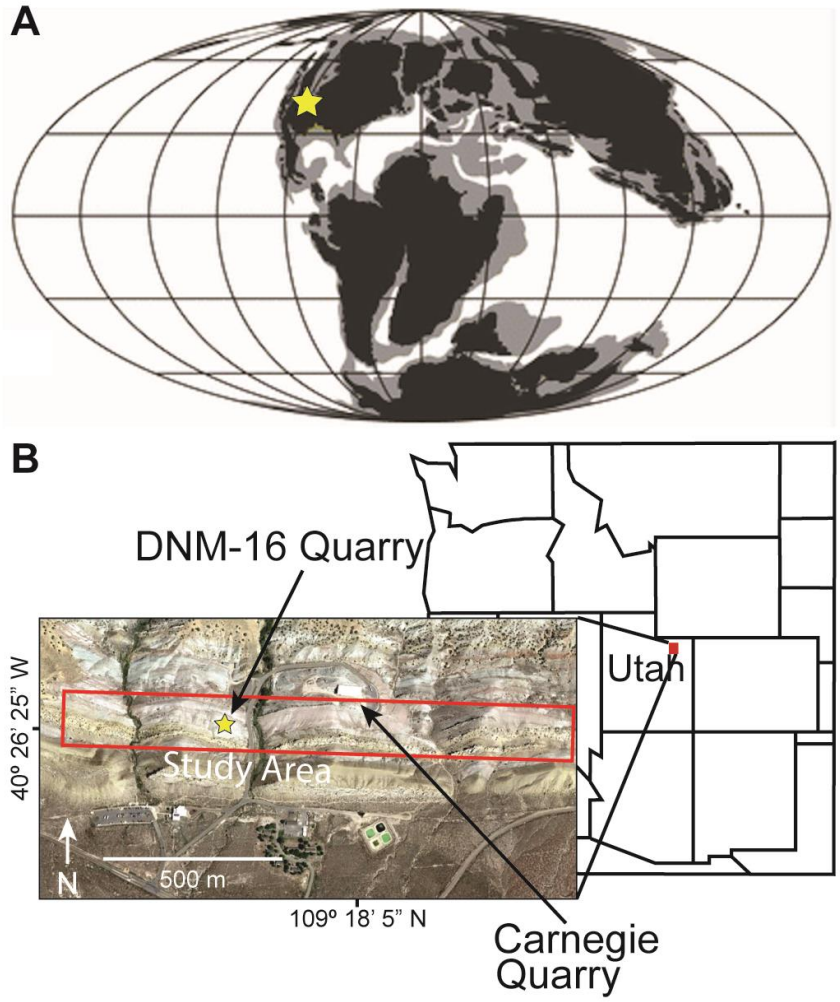

Fig. 1. DNM-16 Locality map. A) Paleogeographic location of DNM-16 during the late Albian, modified from Chure et al., 2010. B) Aerial view of DNM-16 at Dinosaur National Monument in relation to the western United States. Red box denotes study area. Photo source: Dinosaur National Monument, 109°18'5" N and 40°26'25" W Google Earth. May 29, 2017.

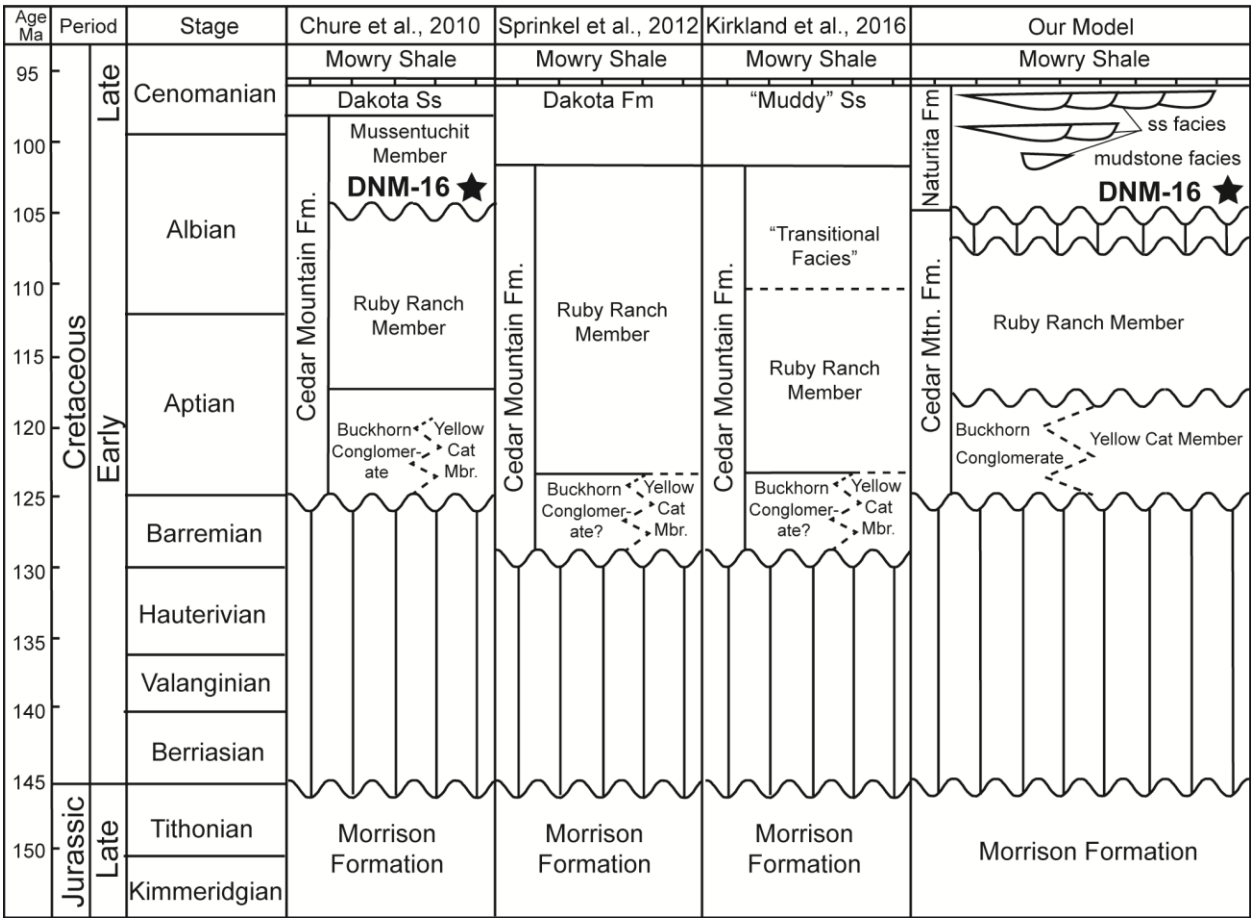

Fig. 2. Generalized stratigraphic models of the Dinosaur National Monument area. Modified stratigraphic columns from Chure et al. (2010), Sprinkel et al. (2012), and Kirkland et al. (2016).

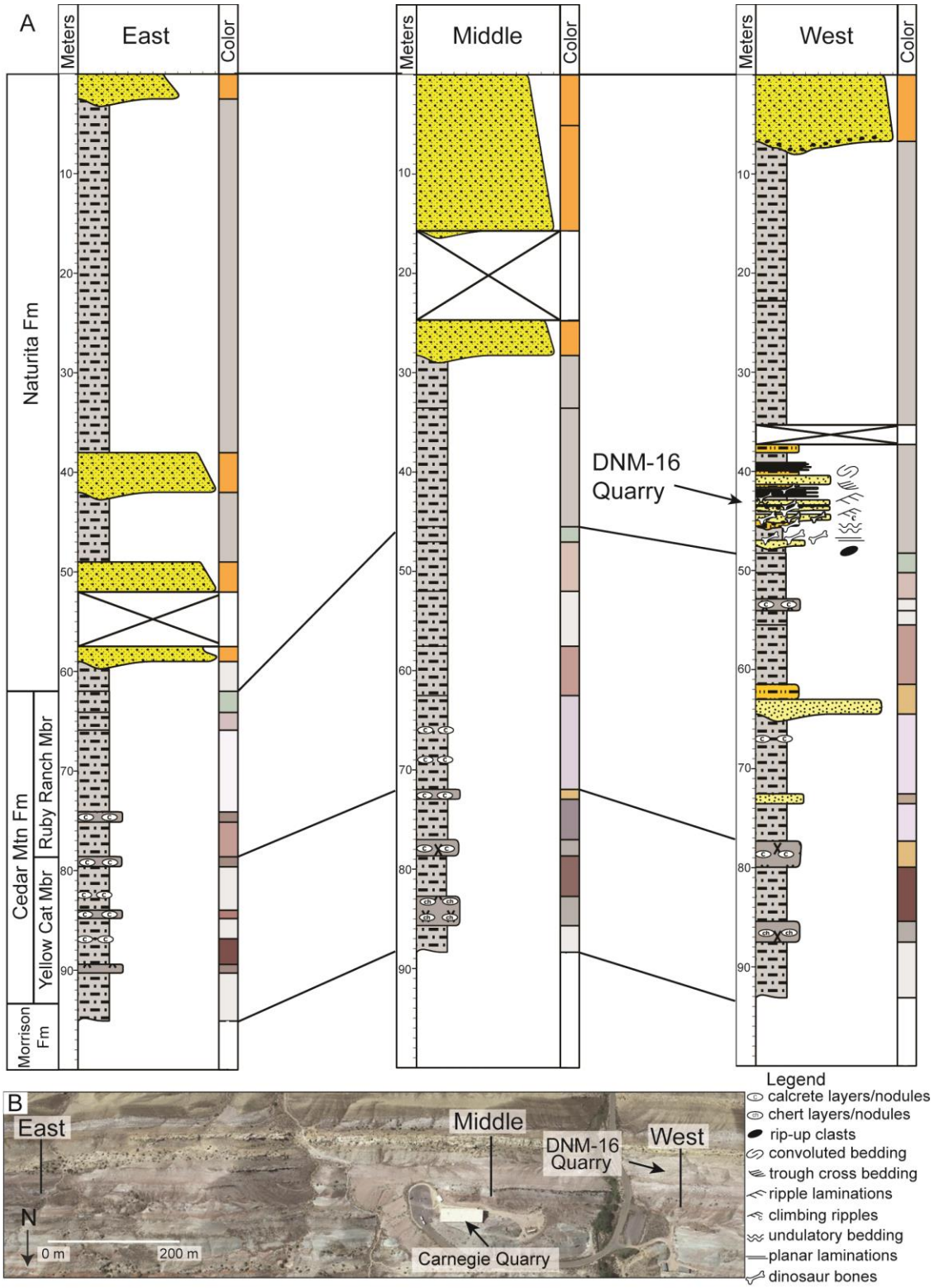

Fig. 3. Stratigraphic columns of the DNM-16 study area. A) Stratigraphic columns from East to West. B) Aerial map correlating the location of the three measured sections. Photo source: Dinosaur National Monument, 109°18'5" N and 40°26'25" W Google Earth. May 29, 2017.

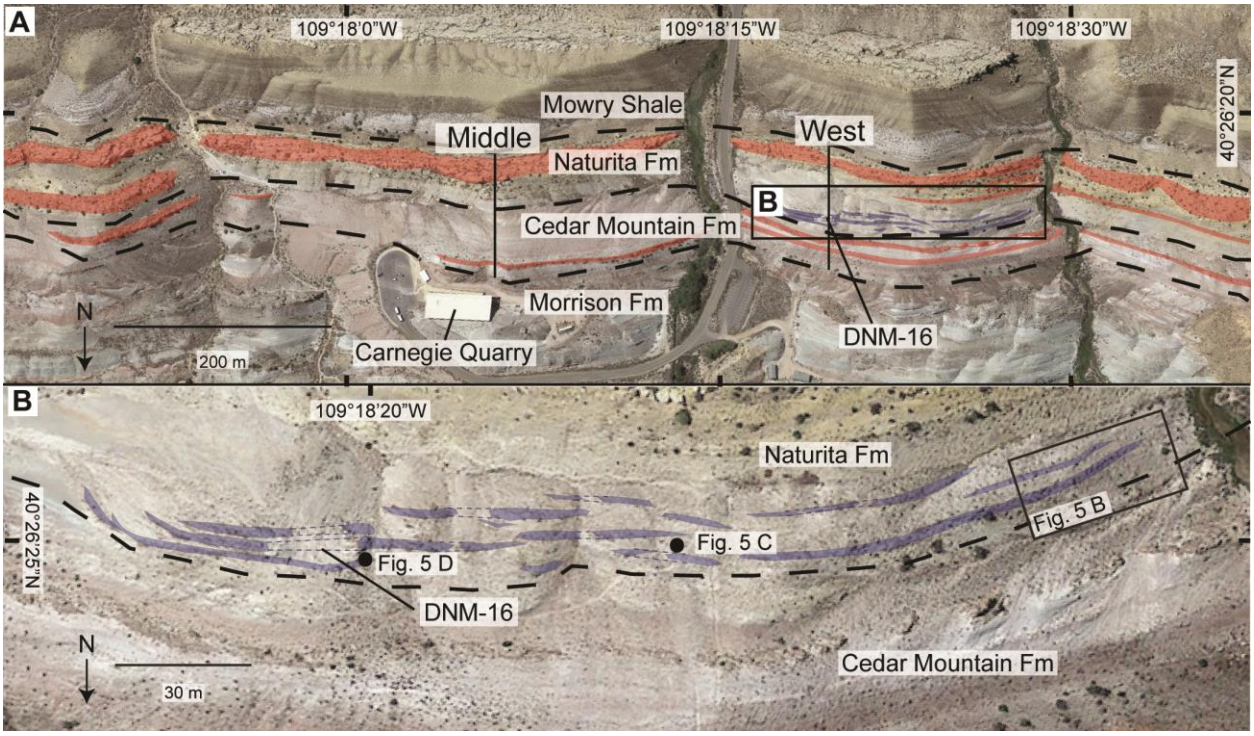

Fig. 4. Plan view of the quarry and surrounding area. A) DNM-16 channels in B emplaced with the surrounding channels of the Cedar Mountain and Naturita formations. B) DNM-16 quarry channels and associated sandstone channels and their general morphology, as well as photo locations for Fig. 5A-B, and D. Slight vertical exaggeration due to oblique photo angle. Note: north is down in this figure to show the top as stratigraphic up. Photo source: Dinosaur National Monument, 109°18'5" N and 40°26'25" W Google Earth. May 29, 2017.

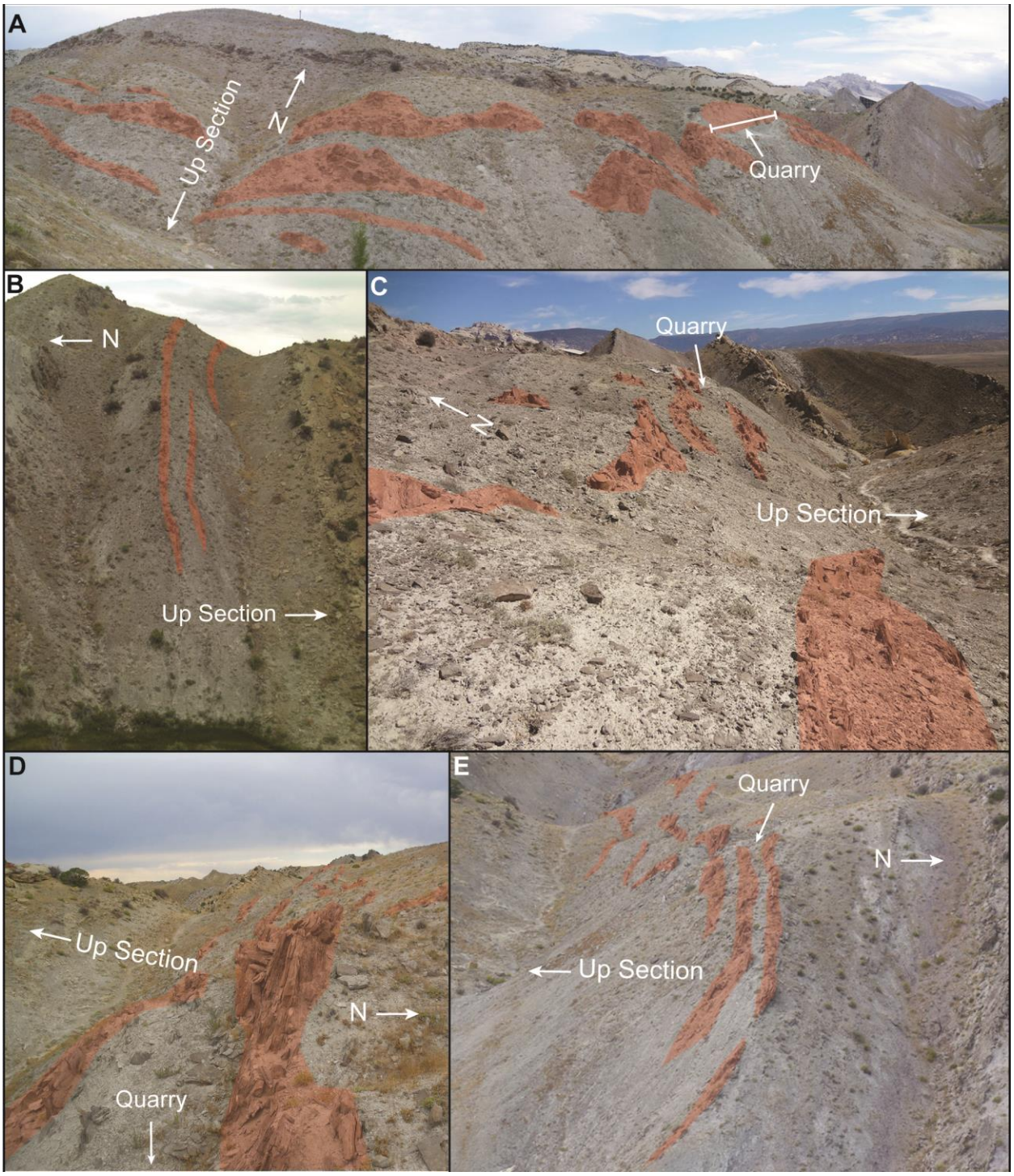

Fig. 5. Outcrop view of the DNM-16 sandstone lithofacies highlighted in red. Channel thickness ranges between 0.5 m and 2 m. A) Looking north from the top of the Naturita Formation. B) Looking east from the west side of the hill; the channels pinch out and cannot be seen any further west (refer to Fig. 4B for reference). C) Looking east toward the quarry from the west side of the channel complex (refer to Fig. 4B for photo location). D) From the quarry looking west (refer to Fig. 4B for photo location). E) South of Carnegie quarry looking west. A-E display the thin, poorly defined sandstone channels as well as the lateral discontinuity.

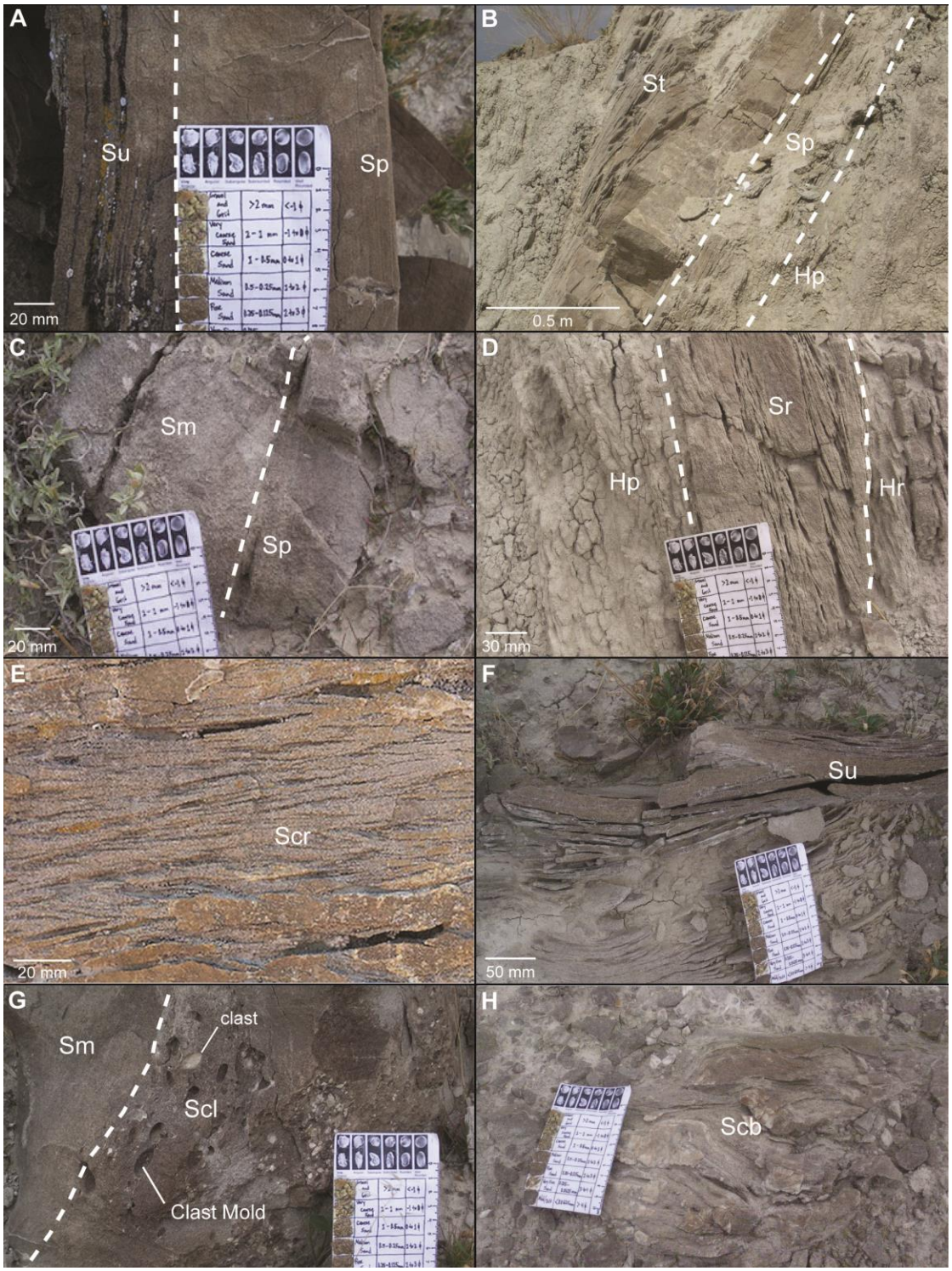

Fig. 6. Sandstone and heterolithic lithofacies from the DNM-16 quarry beds. A-H, sandy lithofacies and some heterolithic lithofacies with the following abbreviations: Sp) sandstone with planar laminations, St) sandstone with trough cross bedding, Sm) massive sandstone, Sr) sandstone with ripple laminations and/or flaser like bedding, Scr) sandstone with climbing ripple laminations and/or flaser like bedding, Su) sandstone with undulatory bedding, Scl) sandstone with rip-up clasts, Scb) sandstone with convoluted bedding, Hp) heterolithic with planar laminations, Hr) heterolithic with ripple laminations and/or wavy like bedding.

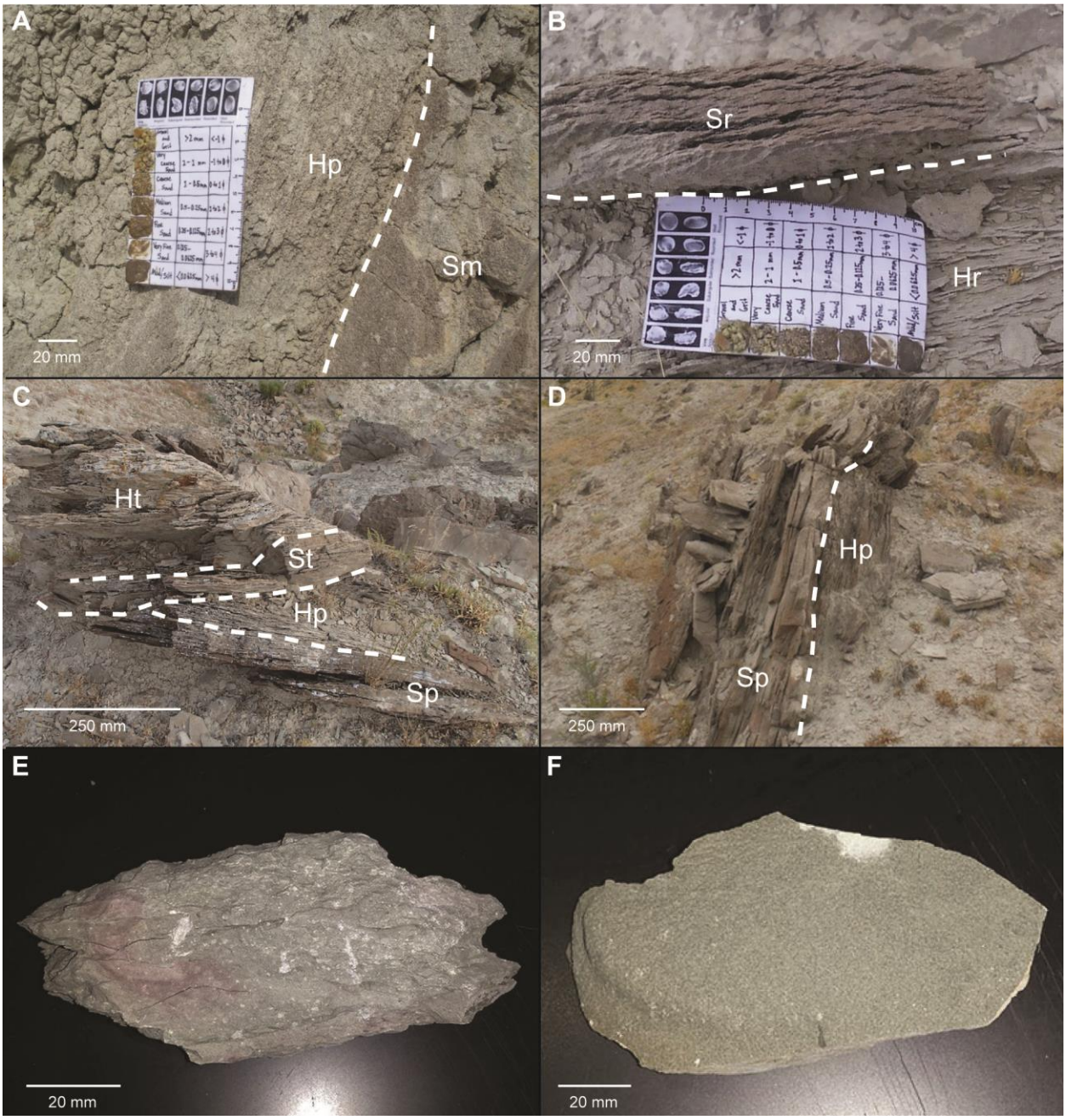

Fig. 7. Heterolithic and sandstone lithofacies from the DNM-16 quarry. A-D, heterolithic lithofacies and some sandstone lithofacies with the following abbreviations: Sp) sandstone with planar laminations, St) sandstone with trough cross bedding, Sm) massive sandstone, Sr) sandstone with ripple laminations and/or flaser like bedding, Hp) heterolithic with planar laminations, Hr) heterolithic with ripple laminations and/or wavy like bedding, Ht) heterolithic with trough cross bedding. E) The Mp lithofacies with weak planar laminations and Stage I gypsum snowballs. F) The Mn lithofacies as a homogenous grey/green siltstone.

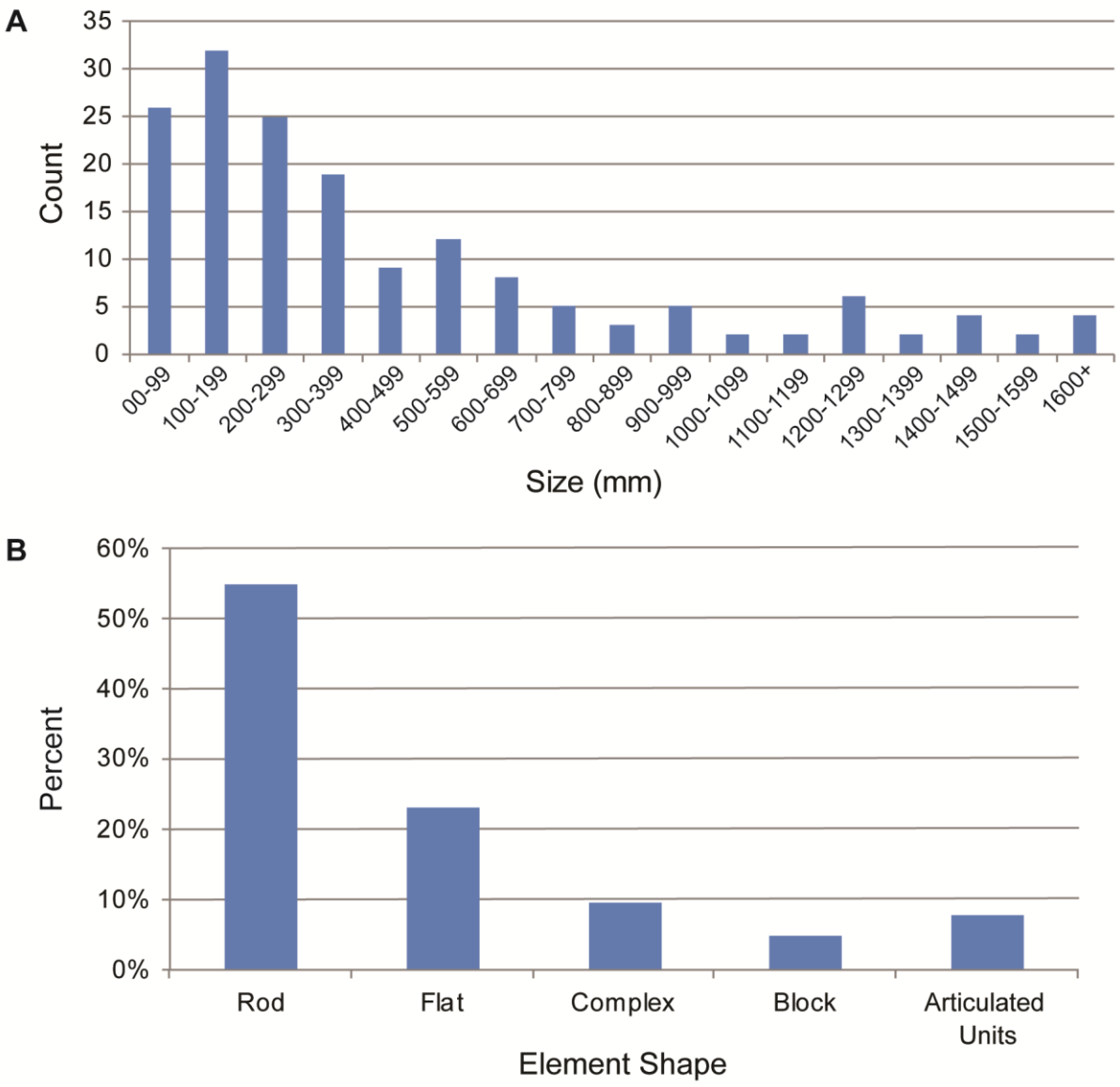

Fig. 8. Size and shape histograms of *Abydosaurus* elements (n=170). A) Size distribution of cataloged elements. B) Element shapes distribution.

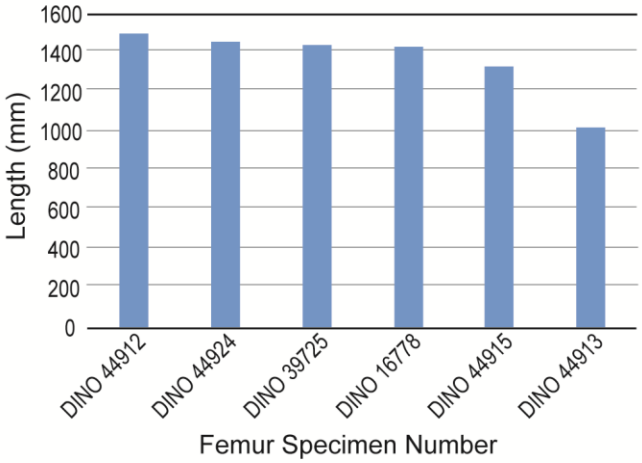

Fig. 9. Femur lengths. Lengths from 6 of the 7 left femora found within DNM-16 (the 7th femur, DINO 44916, was not collected). The lengths are comparable except for femur DINO 44913.

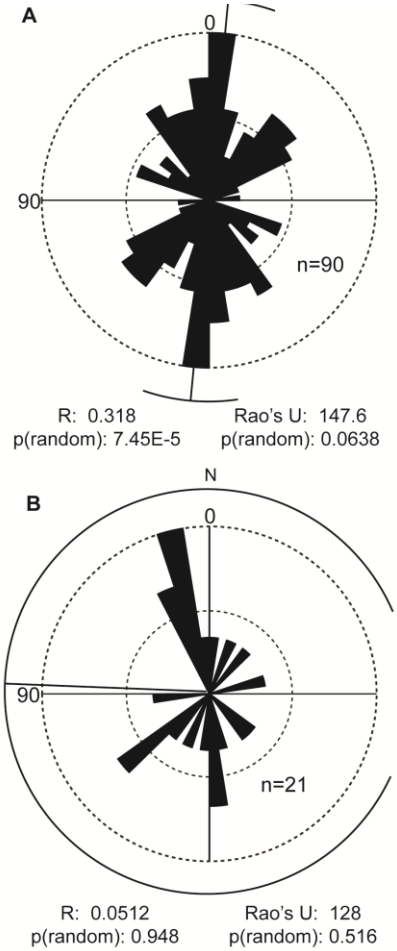

Fig. 10. Bone and articulated segment orientation. A) Bone and articulated segment orientations. B) Vector measurements on long bones and articulated units based on assumptions that the smallest end of a bone or articulated unit points downstream.

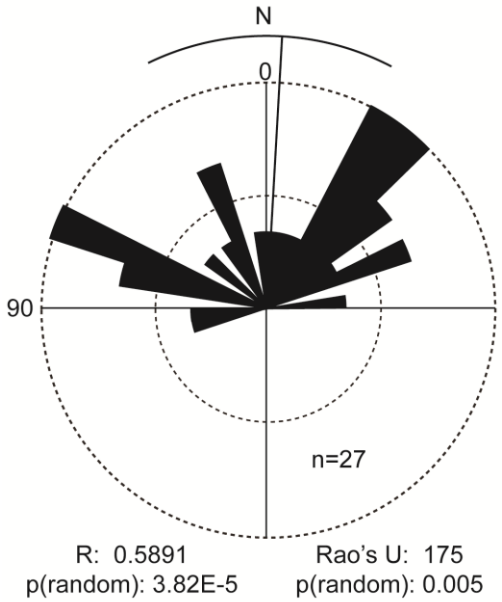

Fig. 11. Paleocurrent measurements from DNM-16 channel bedforms.

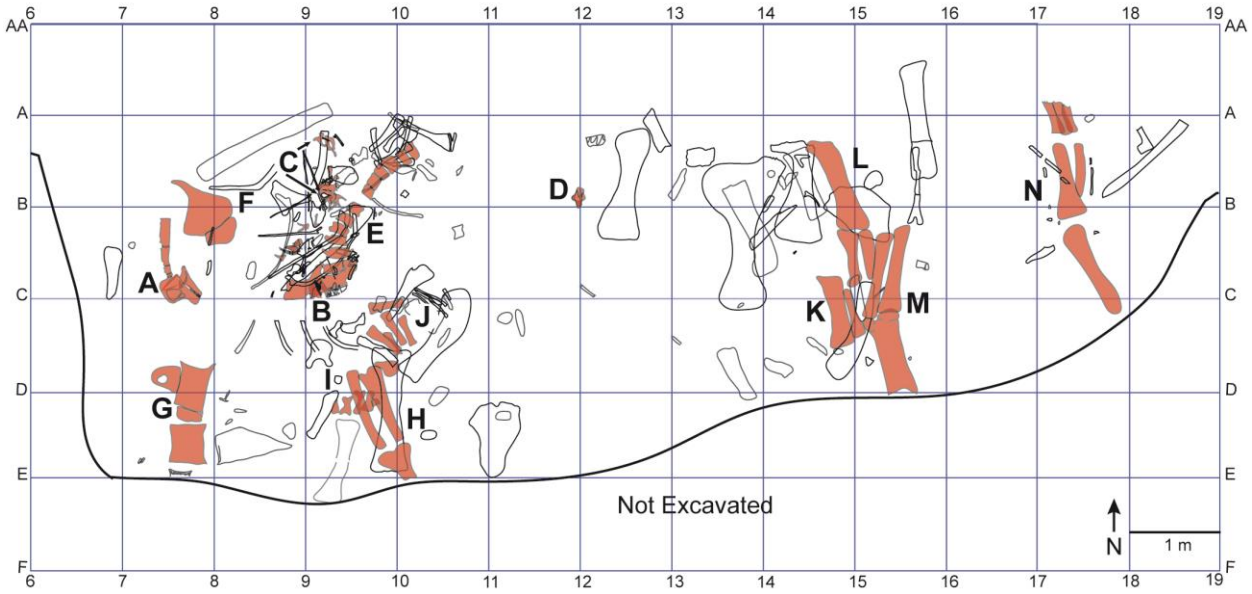

Fig. 12. Quarry map of DNM-16, emphasizing skull elements, articulated and closely associated elements (shown in red). All elements pertain to *Abydosaurus*, except for two shed theropod teeth. A) Holotype of *Abydosaurus mcintoshi*, articulated skull and cervical vertebrae. B) Articulated skull, part lost to collecting. C) Disarticulated skull, nearly complete. D) Isolated braincase. E) Partial pelvis with articulated sacral vertebrae and associated and articulated caudal vertebrae. F) Partial scapulocoracoid. G) Two articulated cervical vertebrae of a larger individual. H) Articulated hindlimb associated with I) articulated metatarsals. J) closely associated metacarpals. K) partial articulated hindlimb. L) articulated hindlimb. M) articulated hindlimb. N) articulated forelimb. Grid squares represent 1 m^2.

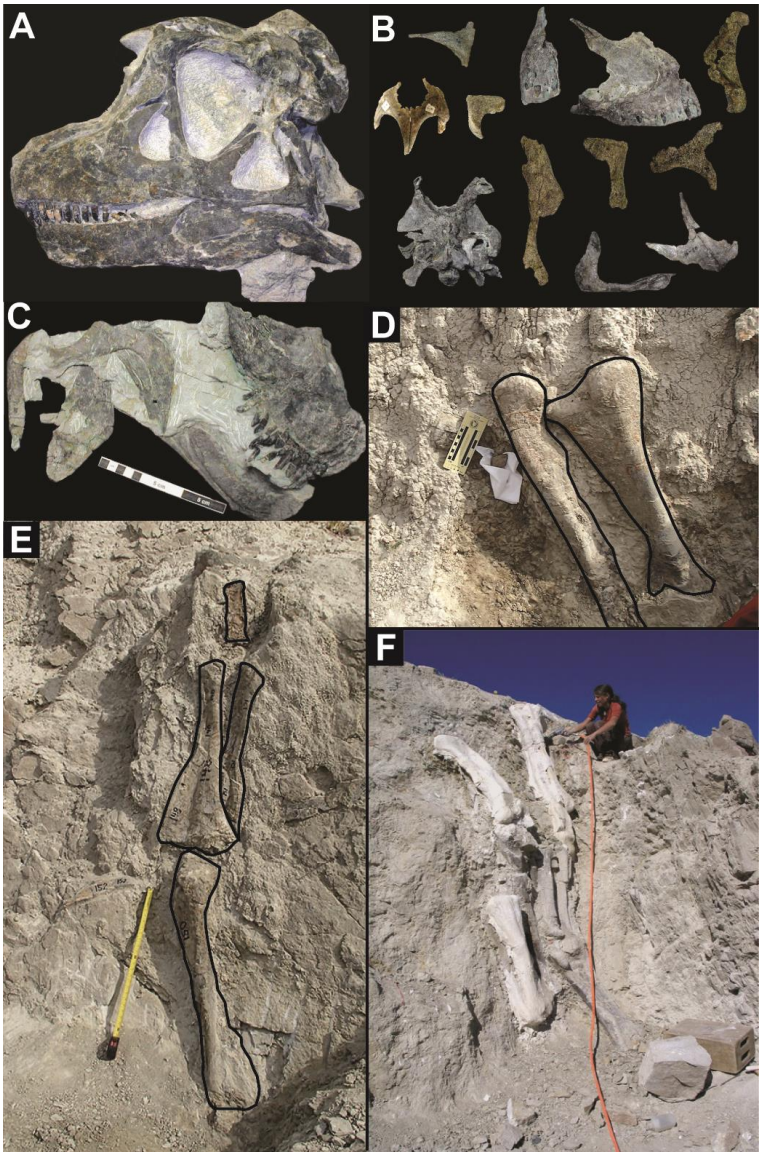

Fig. 13. Skulls and articulated limbs of *Abydosaurus mcintoshi*. A) *Abydosaurus* skull, part of the holotype DINO 16488. This skull includes stapes, hyoid elements, and some sclerotic rings. See Fig. 12A. B) Part of an almost completely disarticulated skull, DINO 17849. See Fig. 12C. The only articulated elements were the braincase and the maxillary and premaxillary teeth which were found as a set of "dentures" (teeth in order as in life but the teeth were not in the maxilla or premaxilla. C) Skull consisting of an articulated rostrum and dentaries with posteroventral elements disarticulated, DINO 17848). D) Hind limb found fully articulated (DINO 44916). See Fig. 12H. E) Largely articulated front limb with the humerus at bottom and a metacarpal at the top of the image (DINO 44917). See Fig. 12N. Two other metacarpals were previously collected, but phalanges were uncommon and never found in articulation. F) Three articulated and aligned limbs (DINO 44913, DINO 44915, and DINO 44922). The bone-bearing lithosome dips at about 68°S, and the bones in the quarry, including D-E are preserved parallel to the bedding plane.

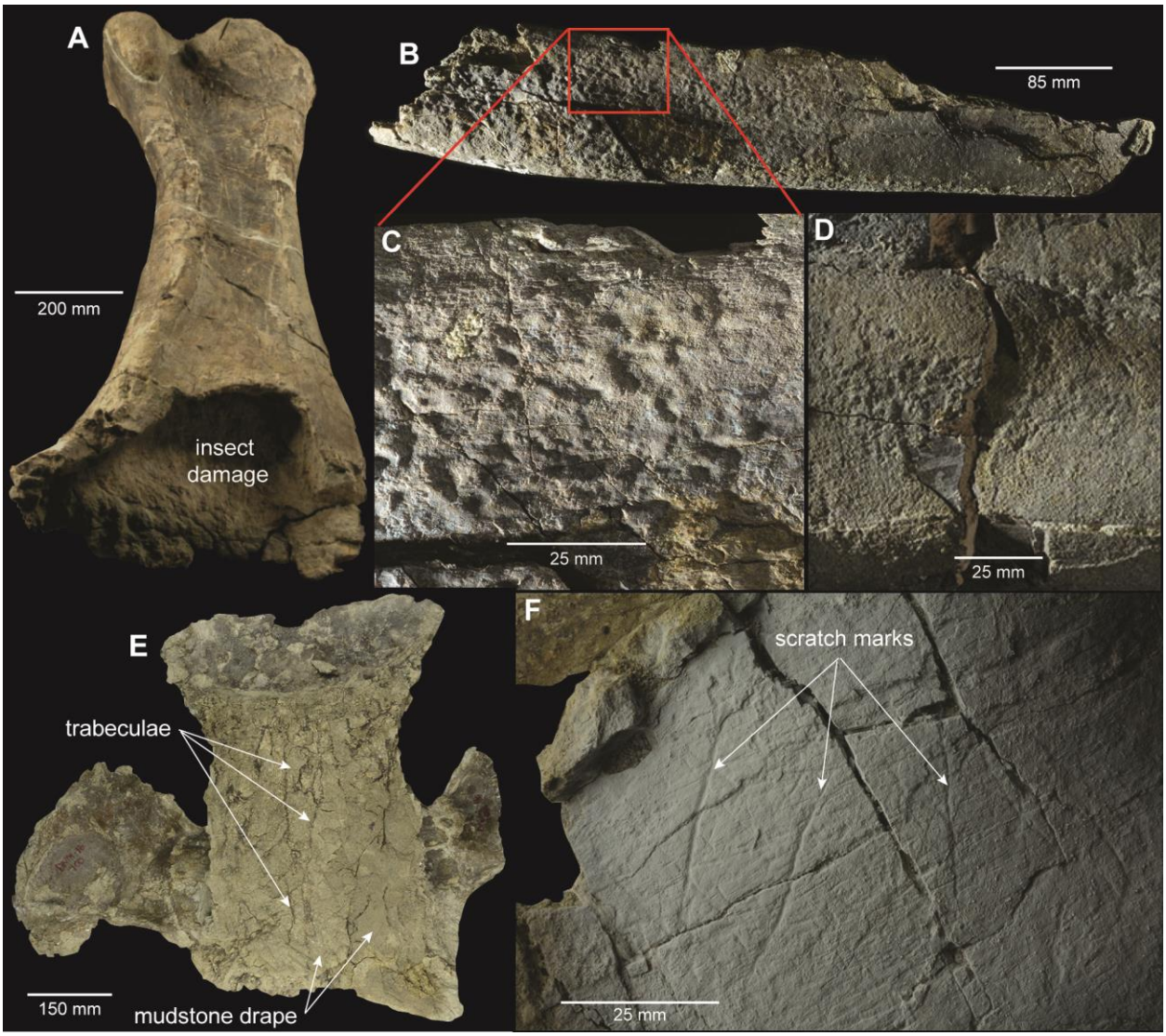

Fig. 14. Bone surface modification of *Abydosaurus mcintoshi* bones. A) Deep pit near proximal end of left femur, DINO 44915. Extreme bone loss is attributed to termite consumption of the articular end and trabecular bone. B) Dorsal rib covered with termite pits (DINO 44923). Box indicates area enlarged in C) Detail of termite pitting. D) Termite pits on femur, DINO 44913. E) Cervical vertebra, DINO 44914, in dorsal view. Upper surface of centrum truncated by fluvial scouring. Select internal trabeculae of what was the pneumatized interior of the centrum indicated by arrows. Post scouring, the trabeculae were covered with mud, which is still present in bottom right. F) Probable tooth scratch marks on blade of scapula, DINO 44921.

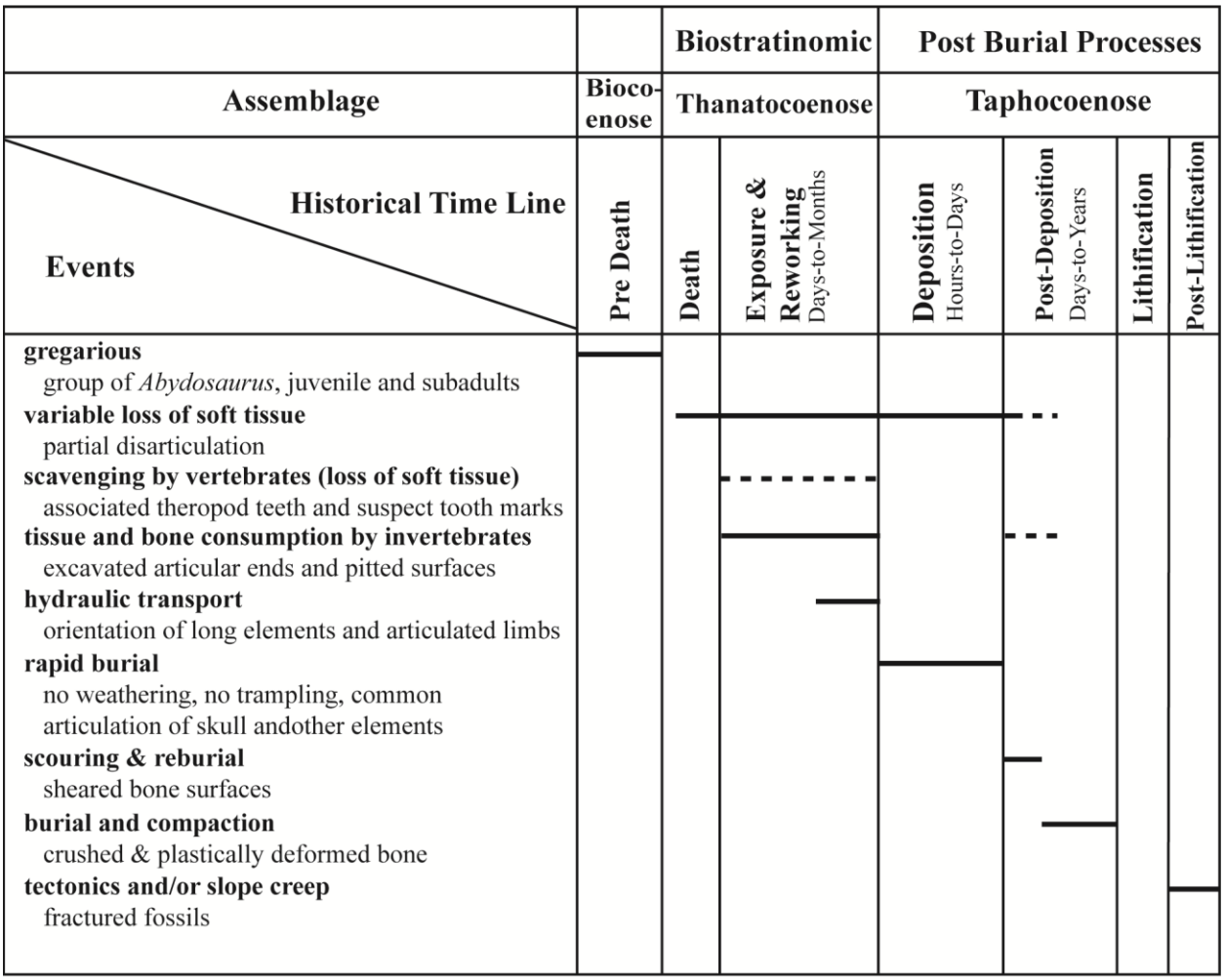

Fig. 15. Taphogram for DNM-16 quarry showing hypothesized sequence and duration of the events.

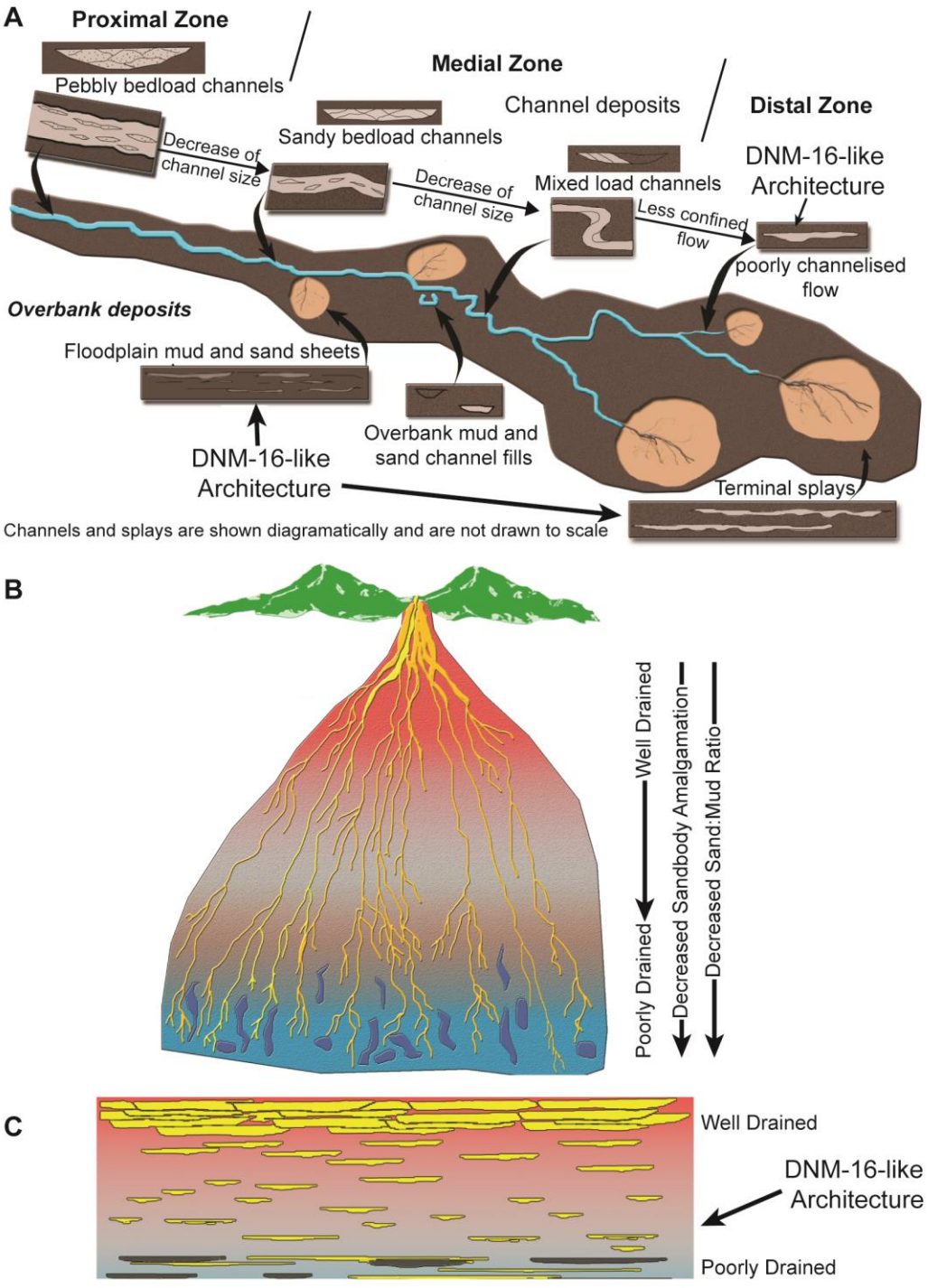

Fig. 16. Distributary fluvial system models. A) Proximal to distal trends in channel form and size in a distributive fluvial system noting likely matches for DNM-16 channel architecture. Distance from illustrated proximal to distal portions is likely tens of kilometers. Modified from Nichols and Fisher, 2007. B) Schematic plan view of a distributive fluvial system showing proximal to distal trends. Active channel belt in yellow; abandoned channel belts in orange; muddy deposits inferred between the channel belts and shown in reds and grays; wetland/lacustrine in blue. C) Schematic cross section of a hypothetical distributive fluvial system from proximal (top) to distal (bottom) ends and the postulated position of DNM-16 within the system. Sandstones in yellow; wetland/lacustrine in dark gray; No vertical scale inferred. Modified from Weissmann et al., (2013).

TABLES

Table 1
Description of facies found within the DNM-16 quarry beds.

Lithofacies	Description	Interpretation
Sm	Mainly fine to medium sand; massive and structureless	Rapid sedimentation and somewhat homogenous composition; bioturbation
Sp	Mainly fine to medium sand; planar laminations	Deposition occurring in the lower flow regime
Sr	Mainly fine to medium sand; ripple laminations and flaser-like bedding	Deposition occurring in the lower flow regime with a rapid decrease in flow velocity and capacity
Scr	Mainly fine to medium sand; climbing ripples and flaser-like climbing ripples	Rapid sedimentation from a rapid decrease in flow velocity and capacity
St	Mainly fine to medium sand; trough cross stratification	Subaqueous dunes
Su	Mainly fine to medium sand; undulatory bedding	Scour and fill structures indicating variations in flow velocity and turbulence within a single flow
Scl	Mainly fine to medium sand; clay, silt, and mud rip-up clasts	Scouring of floodplain mudrock and redeposited near the base of the flow
Scb	Mainly fine to medium sand; convoluted bedding, wavy lamina, and dish/pillar structures	Rapid sedimentation; water is trapped and destroys primary bedding as water escapes during sediment loading
Hp	Fine sands with >20% mud content; planar laminations	Lower flow regime as remaining sand, mud, silt fall out of suspension as the flow terminates
Hr	Fine sands with >20% mud/clay content; ripple laminations or wavy-like bedding	Lower flow regime as remaining sand, mud, silt fall out of suspension as the flow terminates
Ht	Fine sands with >20% mud/clay content; trough cross stratification	Presence of dunes
Mp	Grey mudrock; weak planar laminations, smectitic clay, and pedogenic gypsic snowballs	floodplain mud and clay with evaporitic paleosol development
Mn	Homogenous grey silty mudrock; breaks in smooth nodules and has very little clay content	Distal deposition/settling in stagnant fluid

Table 2
Taxa from DNM-16 and their associated elements.

Taxon	Element
Abydosaurus Mcintoshi	Astragalus
	Atlas
	Chevron
	Coracoid
	Femur
	Fibula
	Gastrolith
	Humerus
	Metacarpal
	Metatarsal
	Phalange
	Radius
	Rib, Cervical
	Rib, Dorsal
	Scapula
	Skull (Complete)
	Sternal
	Tibia
	Tooth
	Ulna
	Vertebra,Caudal
	Vertebra, Cervical
Unknown Theropod	Astragalus
	Phalange
	Tibia
	Tooth